# The hot GDR revisited

Domenico Santonocito, Yorick Blumenfeld

Eur. Phys. J. A (2020) 56:279
https://doi.org/10.1140/epja/s10050-020-00279-6

THE EUROPEAN PHYSICAL JOURNAL A

Review

# The hot GDR revisited

**Domenico Santonocito**[1,a], **Yorick Blumenfeld**[2]

[1] INFN - Laboratori Nazionali del Sud, Via S. Sofia 62, 95123 Catania, Italy
[2] IJCLab, CNRS/IN2P3, Université Paris-Saclay, 91405 Orsay, France

Received: 17 July 2020 / Accepted: 24 September 2020

Communicated by Nicolas Alamanos

**Abstract** The properties of the Isovector Giant Dipole Resonance are reviewed as a function of the temperature of the state on which it is built. The experimental methods, based on scintillation detectors efficient for the detection of high energy gamma-rays, are described. Methods for determining the excitation energy and temperature from the measurement of light charged particle energy spectra taking pre-equilibrium emission into account are presented. The resonance properties, energy, width and strength, are followed as a function of increasing temperature. The data are analyzed in the framework of the statistical model, which is briefly presented, by using the codes CASCADE and DCASCADE. Various prescriptions for the characteristics of the resonance as well as theoretical models are incorporated into these statistical codes in view of a direct comparison with the data. The successes and deficiencies of the Thermal Shape Fluctuation model at low temperatures are discussed. A salient feature is the surprisingly abrupt disappearance of dipole strength above a limiting temperature which depends on the nuclear mass. Several models taking into account the competition between the time scales of collective degrees of freedom and nuclear lifetime only roughly reproduce the trend of the data. This disappearance of strength is tentatively linked to the nuclear liquid–gas phase transition.

## 1 Introduction

Giant Resonances (GR) are a general property of nuclei which consist in a collective excitation of nucleons. In a hydrodynamic model they are viewed as a high frequency vibration around the equilibrium density or shape of the nucleus. Microscopically, they can be described as a coherent superposition of particle-hole excitations. Numerous types of GR excitations exist which can be categorized according to their multipolarity $L$, their isospin $T$ and their spin $s$. A GR is described by three observables, its centroid energy $E$, its width $\Gamma$ and its strength $S$ expressed as a percentage of the corresponding sum rule. A detailed presentation and discussion of GRs can be found in [1,2].

The first GR was discovered in 1947 through photo-fission experiments [3] and was assigned to the Isovector Giant Dipole resonance (IVGDR) ($\Delta L = 1$, $\Delta T = 1$, $\Delta S = 0$) which corresponds to an out-of-phase oscillation of the protons against the neutrons. Subsequently, the other types of GRs were discovered, often through light hadron (proton, deuteron, alpha-particle...) scattering. A comprehensive picture of the GR landscape is now available which has led to unique knowledge of the bulk properties of the nucleus such as incompressibility or symmetry energy.

All these studies pertain to GRs built on the ground state of nuclei. In 1955 Brink and Axel [4,5] conjectured that GRs could be built on any nuclear state and that the characteristics of such GRs would not depend on the detailed microscopic structure of the said state. This gave rise to the hope of studying the properties of GRs built on excited states, so-called GRs in hot nuclei. However, it remained to find a method to experimentally access such GRs which cannot be observed through traditional photo-nuclear reactions or hadron scattering. The breakthrough came from the development of scintillator detectors exhibiting high efficiency for high energy $\gamma$-rays. Indeed, the IVGDR, located above the particle emission threshold, while decaying mainly through light particle emission exhibits a sizeable gamma decay branch (generally between $10^{-3}$ and $10^{-5}$) towards the state upon which it is built. Therefore, starting in the early eighties, numerous studies of high energy $\gamma$-ray emission in fusion reactions were undertaken, which have led to a detailed understanding of the properties of the IVGDR as a function of temperature. This saga is the subject of the present paper. It should be noted that the study of GRs at finite temperature has been limited to the IVGDR, which is the only GR to exhibit such a large $\gamma$ decay rate. Attempts were made to study the Isoscalar

[a] e-mail: santonocito@lns.infn.it (corresponding author)

Published online: 04 November 2020

Giant Monopole Resonance (ISGMR) built on excited states through $e^+e^-$ decay, but were unfortunately unsuccessful [6].

The study of the "hot GDR" is an elegant demonstration of the richness of concepts at work in Nuclear Physics and can be viewed as a vibrant illustration of an advanced Nuclear Physics course. Throughout this paper there will be discussions of nuclear reaction mechanisms (fusion and incomplete fusion), nuclear bremsstrahlung, collective nuclear excitations, sum rules, nuclear temperature, level densities, statistical models, shape fluctuations, high angular momenta, nuclear time scales, phase transitions, and many more.

Section 2 reviews the experimental methods and instrumentation necessary for the study of the hot GDR. Section 3 gives the basics of the statistical model used for the interpretation of the data. The remainder of the paper is structured to follow the properties of the IVGDR with increasing excitation energy or temperature of the underlying state. Section 4 explores the GDR properties at temperatures below 2 MeV and underlines the successes and shortcomings of the Thermal Shape Fluctuation Model (TSFM) in explaining the data. Section 5 moves to the region between 2 and 4 MeV temperature and focuses on the evolution of the GDR width while underlining the importance of correctly accounting for pre-equilibrium emission. The very high temperature region, where the strength of the GDR is observed to decrease and vanish, is discussed in Sect. 6 in the light of models involving the relative time scales of the vibration and particle emission. A summary is presented in Sect. 7. Other reviews on the subject have been previously published [7–10]. In addition, for other topics addressed via the GDR in hot nuclei such as fission, isospin symmetry and Jacobi transitions the reader could refer to Refs. [11–19].

## 2 Experimental methods

The typical gamma-ray spectrum emitted by a hot nucleus formed in a fusion or incomplete fusion reaction exhibits three main components. At low energies, statistical $\gamma$-rays emitted by the compound nucleus at the end of its decay chain give rise to a steep exponential decay. Gamma-rays from the giant dipole resonance decay appear as a broad bump centered between 10 and 20 MeV depending on the mass of the nucleus. For high bombarding energies above 10 A MeV a third, exponentially decreasing, component appears at high gamma-ray energies which is attributed to nucleon-nucleon brehmsstrahlung in the initial stages of the reaction. The possibility to cover a large energy range and to present an optimal efficiency for high energy gamma-rays are characteristics better exhibited by scintillators than by Germanium semiconductor detectors. The vast majority of the experiments have thus used various scintillation detectors.

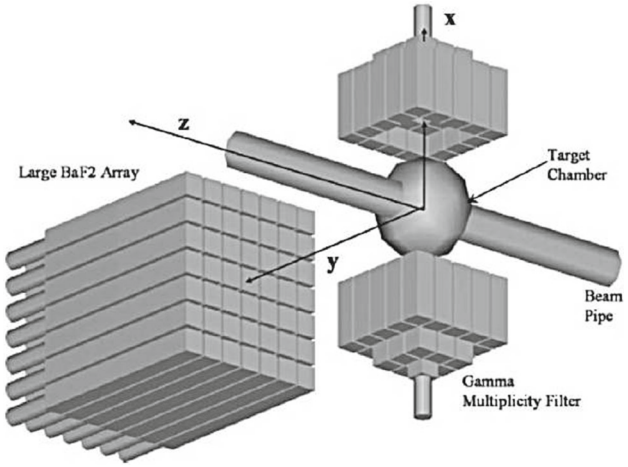


**Fig. 1** Schematic view of the experimental setup for the LAMBDA spectrometer in a 7 × 7 matrix arrangment along with the low energy $\gamma$-ray multiplicity filter [21]

In the early experiments NaI(Tl) detectors were used, mainly because they were readily available. One of the main sources of background in these experiments is due to neutrons which can be separated from $\gamma$-rays by a time of flight measurement and NaI(Tl) exhibits mediocre timing properties. Therefore, the development of $BaF_2$ detectors led to a rapid development of the field. The $\gamma$-ray multiplicity being high in fusion reactions, arrays of a large number of small volume detectors are usually employed in order to limit pile-up. Despite such precautions the response function of the detectors must be measured or simulated. Generally, the statistical calculations are folded with the response function before comparison with the experimental spectra. An example of the measurement of the response of $BaF_2$ detectors to high energy gamma-rays between 20 and 200 MeV is given in Ref. [20] where monochromatic photons of various energies obtained from the in-flight annihilation of positron beams impinged onto the detectors. The experimental response is then parametrized based on Monte-Carlo calculations with the EGS3 code.

In addition to the measurement of the gamma-rays, a delicate point is the determination of the characteristics of the emitting nuclei such as mass, charge, excitation energy, temperature and spin. The nuclei of interest are most often prepared through fusion reactions using heavy ion beams. Below about 5$A$ MeV beam energy complete fusion is the dominant reaction mechanism. In complete fusion reactions the mass and excitation energy are uniquely determined and the spin distribution is triangular from zero to a maximum spin $J_{max}$. Therefore, the experimental setup must allow the discrimination between fusion and peripheral reactions and preferably allow the data to be divided into different bins of spin. Fusion reactions can be signed by requiring a minimum gamma-ray multiplicity since peripheral reactions will have very low

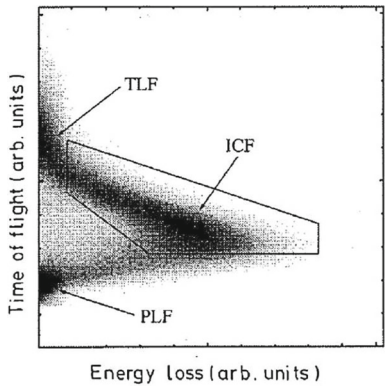


**Fig. 2** TOF–DE plot for heavy nuclei from the $^{36}$Ar + $^{90}$Zr reaction at 27$A$ MeV (from Ref. [22]). Arrows denote target like fragments (TLF), projectile like fragments (PLF) and incomplete fusion residues (ICF) which are selected for the GDR analysis

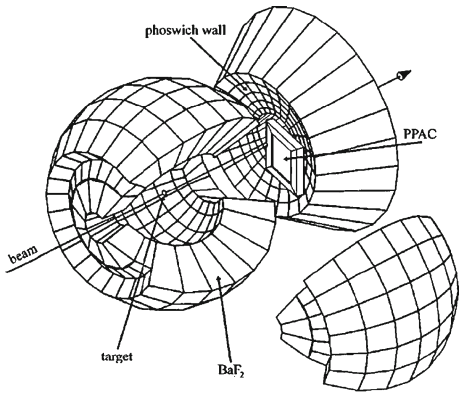


**Fig. 3** Schematic view of the MEDEA detector array and PPAC for residue detections (from Ref. [22])

gamma multiplicity. The initial spin can be estimated event by event using a multiplicity filter since higher initial spins will lead to the emission of a larger number of low energy $E2$ gamma-rays. However, due to inefficiencies and pile-up the number of detectors fired (call fold) is lower than the actual multiplicity, so a given fold will span a certain range of spins which is generally determined by simulations. The multiplicity filter is generally composed of a number of closely packed BGO scintillators for which their low energy resolution is not a drawback for this application. Figure 1 shows a schematic view of a typical set up for such low energy experiments taken from Ref. [21].

If higher excitation energies or temperatures are to be explored, higher beam energies must be used. Complete fusion is then no longer the only reaction mechanism, and in fact completely disappears above approximately 15$A$ MeV beam energy. Incomplete fusion and deep inelastic reactions start to compete and eventually become dominant at the highest energies. It therefore becomes necessary to infer the initial masses, charges, excitation energies and/or temperatures of the emitting excited nuclei. The most frequently used method is to measure the velocity and energy loss of the residual heavy nucleus. This can be accomplished by using fast timing detectors such as Parallel Plate Avalanche Counters (PPAC) where the flight time of the heavy residue is measured between the counter and the beam bunch. Figure 2 shows a typical Time Of Flight vs. energy loss plot for heavy nuclei from Ref. [22]. One can distinguish three regions corresponding to Projectile Like Fragments, Target Like Fragments and Incomplete Fusion Residues, the latter being of interest for the GDR studies. The mass of the composite system, and its excitation energy can be deduced from the velocity by applying a massive transfer model [23]. In this simple but crude reaction model, part of the light partner fuses with the target, while the remainder acts as a spectator, and retains its initial velocity. Different ranges of mass and excitation energy can then be explored by gating on the residue velocity. A refinement to this model can be made measuring the pre-equilibrium particles emitted in the reaction and calculating the correction to be applied to determine the correct excitation energy of the hot compound system [24–26].

If they are placed under vacuum, $BaF_2$ scintillators exhibit the useful property of being sensitive to charged particles as well as gamma-rays. Additionally, their pulse shape is characteristic of the nature of the particle. By integrating the charge signal of the $BaF_2$ in two gates, associated to the fast and slow components of the signal and combining this with a time of flight measurement, gammas, neutrons, protons and alphas can be separated. This was accomplished with the MEDEA detector [27] which is a close to $4\pi$ $BaF_2$ multidetector mounted in a large vacuum chamber. A schematic drawing of MEDEA with the associated PPACs for heavy residue detection is shown on Fig. 3. Another type of setup yielding similar information is displayed on Fig. 4 from Ref. [14] where eight BaF2 scintillators from the HECTOR array detect the high energy gamma-rays, gas-CsI telescopes at intermediate angles detect the light charged particles and two PPAC are placed at forward angles for the heavy fragments. One then extracts charged particle spectra over various angles which can be fit with a moving source prescription. The sources are assumed isotropic and the energy distribution for each source is parametrized, in the source rest frame, adopting a surface-type Maxwellian distribution given by:

$$\frac{d^2M}{d\Omega dE} = \frac{M}{4\pi T^2}(E - E_c)\exp[-(E - E_c)/T] \qquad (1)$$

where $E_c$ is the Coulomb barrier of the particle, $T$ is the source temperature and $M$ is the multiplicity.

In the most general case three moving sources are needed to fit the spectra over the entire angular range. These sources are attributed to emission from a hot projectile-like fragment

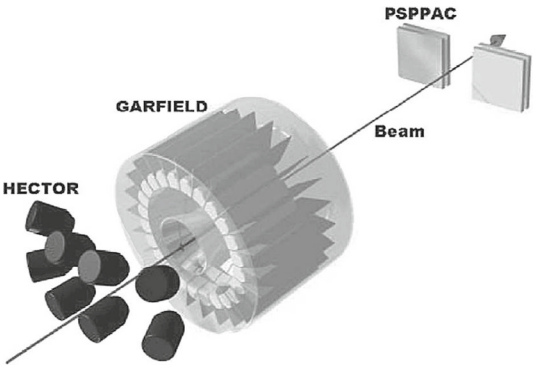


**Fig. 4** View of a typical experimental setup allowing the measurement of gamma-rays (HECTOR), light charged particles (GARFIELD) and heavy fragments (from Ref. [14])

which has not fused, pre-equilibrium emission, and statistical emission from the fused nucleus respectively. The apparent temperature of the fusion-like source is of particular interest since it represents an average temperature of the source over its decay chain. The so-called pre-equilibrium source always exhibits a velocity close to half the beam velocity which corresponds to the nucleon–nucleon center of mass velocity. Knowing $M$ and $T$ of the pre-equilibrium source for each particle type one calculates the energy and mass removed from the system by pre-equilibrium emission in order to infer the initial excitation energy and mass of the equilibrated hot nucleus [26] which will be used as input for the statistical decay calculations. One may also check these initial conditions by realizing a more precise measurement of the evaporation residues.

This was accomplished by combining the MEDEA detector with the SOLE solenoid which selects the residues that then impinge on MACISTE focal plane detector made of two stages gas-plastic scintillator telescopes, as depicted on Fig. 5 [28]. To improve the characterization of the hot residues the MACISTE detector was complemented, in some experiments, with the addition of a few Si–Si telescopes. As an example, the comparison between the $Z$ distribution of residues measured for the $^{116}$Sn + $^{24}$Mg reaction at 23$A$ MeV and a statistical calculation performed using the code GEMINI [29] is shown in Fig. 6. It should be noted that in the high energy reactions the spin distribution is not well defined and difficult to measure and ad hoc assumptions need to be made.

Another mechanism to produce excited nuclei is two body inelastic scattering. Very high excitation energies cannot be reached but the advantages are two-fold. The excitation energy imparted to the target can be precisely known by measuring the kinematic properties of the scattered projectile, for example using a magnetic spectrometer, and the excited nucleus being the target its mass is of course known. In addition, such reactions impart very little spin to the target, so the

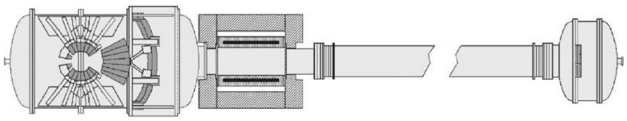

**Fig. 5** Schematic drawing of the multi-detector MEDEA-SOLE-MACISTE setup. MEDEA crystals are placed in the reaction chamber on the left. Next to the MEDEA reaction chamber is placed the solenoid SOLE which allows to convey the reaction products to the focal plane detector MACISTE placed in the reaction chamber on the right end of the figure [28]

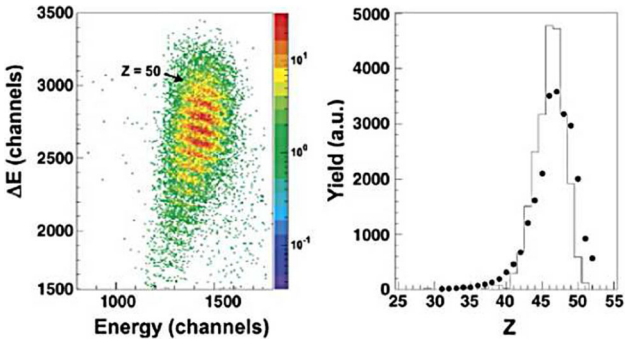


**Fig. 6** Left: $\Delta$E–E plot of evaporation residues from $^{116}$Sn + $^{24}$Mg at 23$A$ MeV; right: $Z$ distribution (points) compared to statistical GEMINI++ calculation using inputs determined as described in text (from Ref. [29])

GDR characteristics can be followed as a function of excitation energy without the influence of increasing spin [30,31].

## 3 Statistical model analysis

Gamma-rays can be emitted at various stages of the reaction both during the first non equilibrated phase (pre-equilibrium) and during all the decay steps of the hot equilibrated system. This implies the emission from nuclei of different masses, charges, spin and excitation energies but also different time scales in the emission processes contributing to the gamma-ray spectra. Above about 8–10 A MeV pre-equilibrium effects start to come into play and become progressively more important with increasing beam energy. Such effects are clearly evident both in the particle and gamma-ray spectra. In the latter a high energy tail appears above the GDR region. Such a contribution, attributed to bremsstrahlung emission from $np$ collisions extends also in the GDR region and must be properly evaluated and subtracted from the spectra in order to obtain the statistical gamma-ray component. This is typically accomplished fitting the high energy part of the gamma-ray spectra ($E_\gamma > 35$ MeV) by an exponential function $Ie^{-(E_\gamma/E_0)}$ having slope $E_0$ and intensity $I$ as free parameters. The extracted slopes exhibit a beam energy dependence which can be reasonably well described by the relation $E_0 = 0.68E_{cc}^{0.83}$ where $E_{cc} = E_{\rm beam} - V_c/A_p$ is the

reduced bombarding energy, $V_c$ is the Coulomb barrier and $A_p$ is the projectile mass [32,33]. The high energy gamma-ray multiplicity $M_\gamma$, obtained integrating the spectra above 35 MeV, reflects the overlap size of the colliding nuclei and can be understood in the framework of a simple geometrical model. In the hypothesis of first chance nucleon-nucleon collisions, the high energy gamma-ray multiplicity is given by the relation $M_\gamma = N_{np}(b) \times P_\gamma$ where $N_{np}(b)$ represents the number of $np$ collisions in the overlap region which is impact parameter dependent and $P_\gamma$ is the probability to produce a bremsstrahlung photon [34]. Complete or close to complete fusion events can be mainly associated to central collisions and using asymmetric reactions a full overlap between colliding nuclei can be assumed to estimate the size of partecipant zone. Within these assumptions the hypothesis of a production of bremsstrahlung photons from first chance nucleon–nucleon collisions gives a reasonably good description of the data.

Since the statistical gamma-ray spectra are not a direct reflection of the gamma emission from the hot system at its initial temperature but rather an average over the whole decay process down to zero temperature, the extraction of the main GDR features is typically performed through a comparison with the results of statistical model calculations assuming as input the excitation energy, mass and charge of the hot system extracted from the data analysis. In the code a triangular spin distribution with a diffuseness of a few $\hbar$ units is typically assumed. In experiments at high excitation energy, due to the saturation of angular momentum, the maximum spin leading to fusion $J_{max}$ is limited at values ranging between 50 and 70$\hbar$ depending on the mass of the system.

In the case of more exclusive measuments using a multiplicity filter also the spin distribution has to be taken properly into account. It can be deduced from the measured fold once the response function of the gamma array to the different multiplicities is known. Different methods have been developed to analyse the gamma-ray spectra measured in coincidence with various fold windows [35–37].

Statistical model calculations are typically carried out using the statistical code CASCADE [38] which treats the statistical emission of neutrons, protons, alphas and $\gamma$-rays from a hot equilibrated system. In a statistical model scenario gamma-rays are emitted in competition with neutrons and light charged particles according to their relative probabilities which depend on effective transmission coefficients and the ratio of initial and final state density. In general, light particle emission from the GDR is much more probable than $\gamma$-decay, but the latter, which has a probability of the order of $10^{-3}$, is a more useful probe of the GDR properties since the $\gamma$-ray carries all the energy of the resonance. The decay rate $R_\gamma$, assuming full equilibration of the giant dipole resonance before the decay, is given by:

$$R_\gamma dE_\gamma = \frac{\rho(E_2, J_2, \pi_2)}{\hbar\rho(E_1, J_1, \pi_1)} f_{\mathrm{GDR}}(E_\gamma) dE_\gamma \qquad (2)$$

where $\rho(E_1, J_1, \pi_1)$ and $\rho(E_2 J_2, \pi_2)$ are respectively the level densities for the initial and final state which differ by an energy $E_\gamma = E_1 - E_2$ and $f_{\mathrm{GDR}}(E_\gamma) \propto \sigma_{abs} E_\gamma^2$. It can be written as:

$$f_{\mathrm{GDR}}(E_\gamma) = \frac{4e^2}{3\pi\hbar mc^3}\frac{NZ}{A} \times \sum_{i=1}^{3} \frac{S_i \Gamma_i E_\gamma^4}{(E_\gamma^2 - E_i^2)^2 + E_\gamma^2 \Gamma_i^2} \qquad (3)$$

where $\sigma_{abs}$ is the E1 photo-absorption cross section which can be represented by a single, double or triple Lorentzian shape, and $S_i$, $\Gamma_i$, $E_i$ are respectively the fraction of the exhausted sum rule, width and energy of each component of the resonance. In the case of spherical nuclei a single Lorentzian is used to reproduce the data while in the case of deformed nuclei retaining an axial symmetry two Lorentzian shapes are typically used. For nuclei showing triaxial shapes three Lorentzian shapes can be used to reproduce the data. From the relative positions of the two GDR centroids, associated to the GDR oscillations along the different axes, a nuclear deformation parameter can be extracted [7]. Comparing Eq. 2 with the neutron emission rate calculated in the framework of the statistical model it follows that high energy gamma-ray emission is favoured to occur in the first steps of the decay process. Therefore the GDR gamma-rays essentially reflect the GDR properties in the hot system populated in the reaction while the low energy part of the gamma-ray spectrum, below about 8 MeV, is mainly emitted at the end of the decay process [7].

A crucial role in the calculation of the decay rate, as shown by Eq. 2, is played by the nuclear level density. At low excitation energies, calculations are typically performed using a fixed level density parameter $a$ ranging between $a = A/8$ and $a = A/9.5$ during the entire decay sequence. With increasing excitation energies the level density parameter has been observed experimentally to decrease to $a = A/12$–$A/13$ [39]. Therefore a proper reproduction of the gamma-ray spectra within the statistical model, especially in the case of high temperatures (above $T = 2$–$2.5$ MeV) calls for the inclusion of parametrizations describing the evolution of the level density parameter as a function of energy. In the past specific parametrizations have been sometimes included in the code by the authors. A recent version of the code CASCADE called DCASCADE, developed by Diosegi [40], uses a different formula for the nuclear level densities that allows to reproduce the evaporation residue, gamma-ray and neutron data simultaneously [40]. The original version of CASCADE treats the level density parameter $a$ and $\Delta$, the pairing energy, separately in different regions of excitation energy.

Below $E^* = 10$ MeV the code uses the Dilg et al. [41] parametrizations for $a$ and $\Delta$ while for $E^* > 20$ MeV the level density parameter $a$ is parametrized as $a = A/K$ (liquid drop value) where $K$ is an input parameter. $\Delta$ is calculated internally by the code assuming that the virtual ground state for the level density in this region should coincide with the ground state energy of a spherical liquid drop without shell and even-odd corrections. In the region $10 < E^* < 20$ MeV a linear interpolation between the two parametrization is carried out. DCASCADE instead uses the Reisdorf formalism of Ignatyuk for the level density description [42,43]. At very low excitation energy this parametrization includes the nuclear structure shell effects and smoothly evolves towards the Fermi gas values at higher excitation energies. Similarly to the Pulhofer version, the level density parameter $a$ is defined as $a = A/K$ where $K$ is an input parameter. However, different parametrizations for the level density parameter as a function of the temperature of the hot system which reproduce the experimentally observed trend were also implemented in code.

In a few recent cases a modified version of GEMINI++ [44,45] properly including gamma-ray emission and level density parametrization was also used to reproduce the experimental gamma-ray spectra [46].

In order to compare the statistical model calculations with data the calculations have to be folded with the detector response. From the comparison the GDR parameters are extracted through a $\chi^2$ minimization procedure which uses the GDR parameters as free parameters. Data taken in different mass regions and in a wide range of excitation energies have shown that the resonance energy value is mass dependent and it is rather stable with excitation energy. Data up to about $E^* = 200$ MeV can be well reproduced assuming 100% of the EWSR while the width is observed to increase significantly from its ground state value as a function of spin and excitation energy. Despite this experimental evidence, historically most of the calculations were performed assuming a fixed GDR width along the whole decay sequence. More recently, in experiments investigating the GDR properties below $T < 2$ MeV, statistical model calculations were also performed including parametrizations of the GDR width as a function of excitation energy and spin [31,47,48].

The comparison of the main GDR features with theoretical model predictions calls for a proper definition of the temperature and spin values characterizing the hot system undergoing GDR decay since the experimental quantities extracted from the analysis represent averages over all the steps of the decay process down to the ground state and are lower than values of the initial compound nucleus. The temperature of the nucleus upon which the GDR is built is usually calculated using the expression:

$$T = \frac{1}{[d(ln(\rho))/dE]} \tag{4}$$

where $\rho$ is the level density or alternatively as:

$$T = \left[\frac{(E^* - E_{\mathrm{rot}} - E_{\mathrm{GDR}})}{a}\right]^{1/2} \tag{5}$$

where $E_{rot}$ is the nuclear rotational energy. Different approaches were followed to define the average $T$ and or the average $J$. One approach used defines $\langle T \rangle$ as the value obtained calculating the weighted average of the temperature of all nuclei of the decay process, using as a weight, at each step, the gamma-ray yield in the GDR region. For each nucleus of the decay chain the temperature is calculated using the expression 4 or 5. This approach might lead, especially in experiments at high excitation energies, to an average temperature which would not reflect the GDR width extracted in the fitting procedure since the last steps in the decay process do not contribute significantly to the GDR decay. In fact, it has been observed that applying a significant change in the GDR width in the low temperature part of the decay chain would not affect significantly the result of the fit to the gamma-ray spectra [49–51]. For this reason, an effective temperature $T_{\mathrm{eff}}$ was introduced as the temperature at which about 50% of the total gamma-ray yield is emitted from the hot system in its decay process from its initial conditions. Then the weighted average of the nuclear temperature is calculated only from the initial value down to $T_{\mathrm{eff}}$. Such approach, followed by different authors [21,50], leads to temperatures which are slightly higher than the one obtained from the average of the whole decay sequence, the difference becoming increasingly important with the excitation energy of the hot decaying system. In some cases, at low excitation energies, the temperature was extracted from the excitation energy of the compound system populated in the reactions corrected for the average rotational energy and for the GDR resonance energy [52,53].

## 4 The GDR behaviour at T < 2 MeV

Broad systematics were collected on the GDR properties built on excited states in nuclei up to about 2 MeV temperature. A comprehensive review on this topic both from theoretical and experimental point of view was recently written by Chakrabarty et al. [10]. The main aim of the study of the GDR in this temperature range was to use it as a tool to investigate the nuclear shape evolution and fluctuations associated to the weakening of shell effects and to disentangle temperature induced from angular momentum driven effects.

The first measurements on the GDR built on excited states using heavy ion fusion reactions were performed on $^{122}$Te, $^{150}$Gd and $^{164}$Er by Newton and coworkers in 1981 [54].

However, the systematic investigation on the evolution of the GDR properties built on excited states was initially focused on Sn isotopes (A $\simeq$ 110) which have spherical ground states. In this mass region the GDR is characterized by a centroid energy of about 14–15 MeV, a width of about 5 MeV and a strength fulfilling 100% of the EWSR. The data collected by Gaardhøje et al. up to $E^* = 100$ MeV [55,56] and then extended by Chakrabarty up to 130 MeV [47] showed that the GDR centroid energy was remarkably stable with increasing excitation energy, the strength retained 100% of the Energy Weighted Sum Rule while the width was observed to increase with a trend that could be nicely reproduced assuming an energy dependence given by the relation $\Gamma = 4.8 + 0.0026E^{1.6}$ MeV where the first term represents the ground state value [47]. In these works, all the statistical model calculations performed to extract the GDR parameters assumed a fixed width during the whole decay process. The attempt to include the dependence of the width on the excitation energy in the statistical model calculations, according the previous parametrization, failed to reproduce the spectra at all the excitation energies. They could be reproduced only including also a $J^2$ dependence according to the relation $\Gamma = 4.5+0.0004E^2+0.006J^2$ [47] which shows the influence of both spin and temperature in the observed width increase. In fact, when the nuclear spin increases the nucleus will sample progressively larger shape deformations which will lead, on average, according to the $1/R$ dependence of the resonance energy, to a broader width. At the same time, the increase in the temperature will induce an increase in the thermal shape fluctuations which induce the nucleus to sample diffent shapes. The net effect observed is to wash out the structure of the GDR absorption strength function leading to a broadening and smoothing of the resonance. In order to evaluate the importance of temperature and spin contributions to the width increase, the experimental investigations were undertaken varying one parameter at a time keeping the other fixed.

Studies of spin induced effects on the GDR width were undertaken, populating hot and rotating $^{109,110}$Sn nuclei in a fixed range of temperatures $T = 1.6$–$2.0$ MeV, using fusion reactions [57]. High energy gamma-rays were measured using eight large volume $BaF_2$ crystals (HECTOR array [58]) while an array of 38 smaller $BaF_2$ was used as a multiplicity filter. Gamma-ray spectra associated to average spin values ranging from 40$\hbar$ to 54$\hbar$, deduced from the measured fold distributions, were reproduced assuming a GDR width increasing from 10.8 to 12.8 MeV [57]. This result confirmed previous indications concerning the importance of angular momentum in driving the width increase. The data set on Sn isotopes was extended to lower spins through the study of the reaction $^{56}$Ni + $^{48}$Ti investigated at a bombarding energy of 260 MeV which led to the formation of a hot compound system of $^{106}$Sn at $E^* \simeq 80$ MeV [35]. The analysis of the gamma-ray spectra performed through a comparison

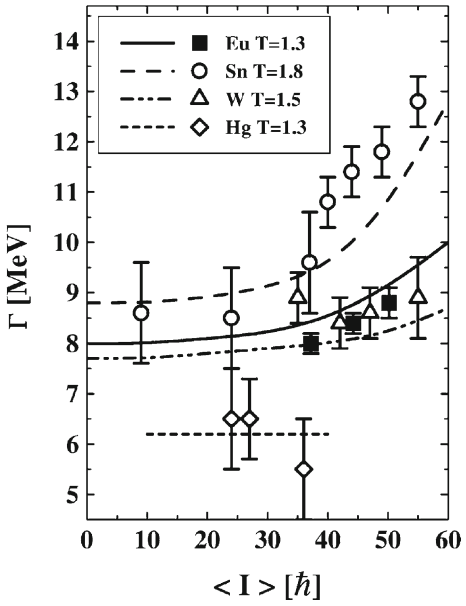


**Fig. 7** Evolution of the GDR width as a function of angular momentum for nuclei in different mass regions (from Ref. [62]). Open circles correspond to Sn isotopes [35,57], open triangles to W isotopes [63], full squares to Eu [62] and open diamonds to Hg [64]. Different lines correspond to thermal shape fluctuation model calculations performed for the nuclei in the different mass regions as shown in the legend

with statistical model calculations allowed the extraction of a GDR width of 8.5 $\pm$ 1 MeV at $\langle J \rangle = 24\hbar$ and of 9.6 $\pm$ 1 MeV at $\langle J \rangle = 36\hbar$. The overall data set on Sn isotopes built at similar temperatures is shown in Fig. 7 as open circles. It shows that in this mass region, the width is fairly constant up to about 35$\hbar$ while above this value a rapid increase as a function of angular momentum is observed [35]. Such a trend of the data is consistent with predictions of TSFM [59–61] for Sn nuclei at an average temperature $T = 1.8$ MeV, shown in the same figure as a dashed line. The model predicts that with increasing excitation energy and spin the nucleus undergoes shape fluctuations and spin driven deformations. Under an adiabatic assumption, shape fluctuations are slow compared to the GDR vibrations which can therefore probe the different nuclear shapes. As a result the GDR width would represent an average of all the frequencies associated with different shapes. With increasing angular momentum nuclear deformation increases rapidly but an effect on the width is observed only when the equilibrium deformation ($\beta_{eq}$) increases sufficiently to affect the mean value of the deformation. The nucleus also experiences a spread in deformations whose value is given by the variance $\Delta\beta = \sqrt{\langle\beta^2\rangle - \langle\beta\rangle^2}$. When the value of $\beta_{eq}$ is smaller than the variance, the mean deformation and the GDR width are not affected significantly. Thermal shape fluctuations play an important role in masking and washing out the effect connected with equilibrium deformation leading to a flat behaviour at low spins.

Complementary works were also performed in other mass regions. Data collected at similar temperatures on $^{147}$Eu [62], $^{176}$W [63] and $^{194}$Hg [64] are shown for comparison in Fig. 7. The effect of angular momentum is observed to decrease as a function of the mass of the hot system. While a small increase in the width is observed at higher spins for $^{147}$Eu and $^{176}$W nuclei, in $^{194}$Hg no effect on the GDR width connected to the spin variation was measured. This can be well understood in the framework of the thermal shape fluctuation model and clearly indicates that the GDR width evolution due to angular momentum effects depends on the nuclear moment of inertia and is driven by the rotational frequency. For a fixed value in spin, the higher the moment of inertia of the nucleus, the smaller will be the effect. This result supports the basic assumption of the thermal fluctuation model, namely that the dipole vibration is not only coupled to the most probable deformation but to the ensemble of the nuclear deformations characterising the nucleus at finite temperature and angular momentum.

However the TSFM is not always able to explain the experimental results. Important discrepancies were found in the study of the reaction $^{28}$Si + $^{124}$Sn at 149 and 185 MeV populating $^{152}$Gd at $E^* = 87$ and $E^* = 116$ respectively [65] and therefore at similar average temperatures. The experiments were focused on the study of the evolution of the GDR width as a function of the spin in the range between about 20$\hbar$ and 60$\hbar$. The extracted width varied from about 8.5 MeV to 10.1 MeV for the lower excitation energy data set while in the study of the same reaction at a beam energy of 185 MeV, the width was observed to increase from 9.5 to 11.7 MeV as shown in Fig. 8. Data were reproduced using the Kusnezov phenomenological formula, which describes the GDR width behaviour as a function of spin and temperature in nuclei where the liquid drop model is valid [61]. It was deduced from a comparison of available experimental results in different mass regions with theoretical calculations that include thermal shape fluctuations in nuclei [61].

The results of the calculations are shown as full and dashed lines in Fig. 8 for both the reactions. Surprisingly the two data sets could not be reproduced with the same value of the parameter $\Gamma_0$ representing the GDR width on the ground state which should be independent of the excitation energy. In fact, fixing this value to fit the results for one beam energy, the same value should also reproduce the data at other beam energies. This result suggested to the authors the existence of a further contribution to the $T$ and $J$ dependencies of the GDR width already included in the TSFM which could be ascribed to the collisional damping of the GDR at higher $T$ [65,66]. Such a phenomenon is essentially connected to the coupling of the GDR to the quantal fluctuation of the nuclear surface. Further data are needed to support this hypothesis.

Temperature induced effects on the GDR width were first investigated using the inelastic scattering of 40$A$ and 50$A$ MeV alpha particles on $^{120}$Sn and $^{208}$Pb targets [30,53]. Gamma-rays were measured in coincidence with scattered alpha particles using an array of 95 $BaF_2$ detectors with a geometrical efficiency of about 10% and the dwarf ball coupled to a wall array made of CsI. Narrow ranges of excitation energy were selected applying a proper gating on the energy loss of the projectile. Gamma-ray spectra were sorted accordingly. The spectra showed a clean bump associated to the GDR decay and a high energy tail due to a non-statistical contribution arising from $np$ bremsstrahlung process. The statistical contribution was reproduced using the CASCADE code assuming for the GDR a width increasing from 5.5 MeV at $T = 1.24$ to 11.5 MeV at $T = 3.1$ MeV in the case of the $^{120}$Sn target. Data on the $^{208}$Pb target were instead reproduced assuming a width increasing from 5.7 MeV at $T = 1.34$ MeV to 8 MeV at $T = 2.05$ MeV [53]. Temperature values were extracted according to Eq. 5 using an excitation energy dependent level density parameter. The measured trend of the width was compared with TSFM calculations which give a reasonable description of the overall GDR width increase as a function of the system temperature in the case of $^{120}$Sn while the $^{208}$Pb data lies rather below the calculations [67,68]. The inclusion of the evaporation width contribution [69] to the GDR width due to the finite width of both initial and final nuclear states involved in the GDR decay improves and extends the agreement between $^{120}$Sn data and theory up to the highest $T$ values. However the calculations are not

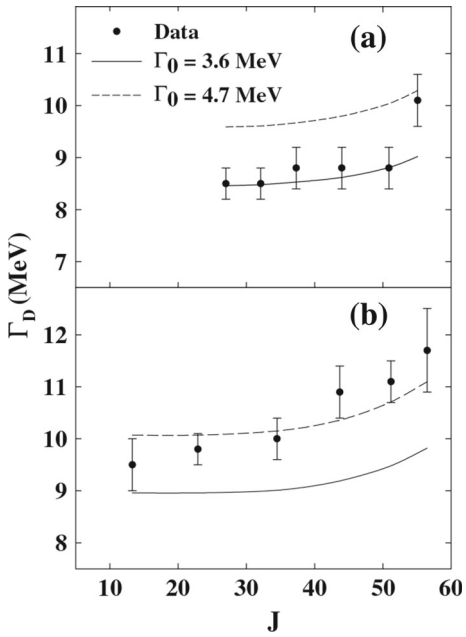


**Fig. 8** GDR width evolution as a function of the average spin for the reactions $^{28}$Si + $^{124}$Sn at 149 MeV (**a**) and at 185 MeV (**b**) beam energy. Solid and dashed lines correspond to the predictions of the Kusnezov parametrization of the TSFM using two different values of the $\Gamma_0$ parameter (from Ref. [65])

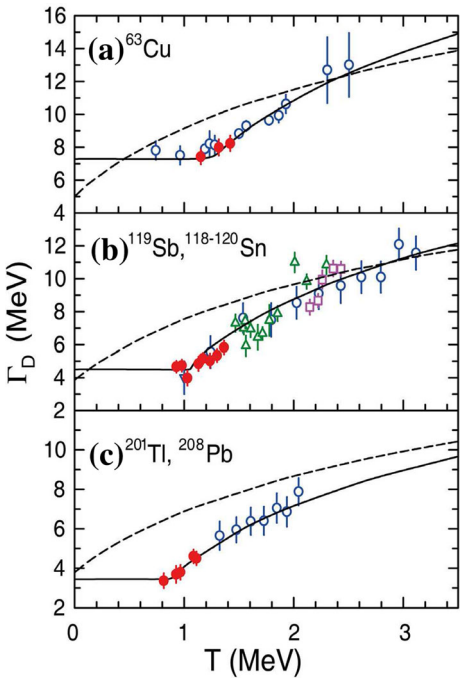


**Fig. 9** Trend of the GDR width as a function of nuclear temperature (from Ref. [72]). Data collected from different experiment are sorted according to the nuclear mass and are shown in different panels. **a** The width trend for $^{63}$Cu. Filled circles are from Ref. [72] while open circles are from Ref. [61,73]. In **b** are collected data on $^{119}$Sb [72] shown as full symbols and on $^{119,120}$Sn nuclei [31,52,53,61]. In **c** data on $^{201}$Tl nuclei [72] are shown as full symbols and on $^{208}$Pb nuclei as open symbols [53]. Full lines represent the predictions of the critical temperature included fluctation model while the dashed ones represent the calculations in the framework of TSFM

able to reproduce the data trend below $T < 1.5$ MeV. One possible reason of this failure was attributed to an improper comparison between data and theory which was performed using the initial temperatures of the compound nuclei. For this reason, a re-analysis of the data, taking into account a weighted average of the temperatures of nuclei contributing to the GDR gamma emission over the various decay steps, was later performed. The comparison of theoretical predictions with data using the new average temperatures showed an improvement in the agreement with $^{208}$Pb data while a clear discrepancy between TSFM predictions and $^{120}$Sn data was observed below about $T = 1.5$–2 MeV [61]. Such discrepancy was then confirmed comparing new data taken in different mass regions with TSFM predictions and could not be attributed to shell effects.

Recently different measurements using either inelastic scattering or fusion reactions were performed to address the problem related to the width trend below $T < 1.5$ MeV [31,61,70–72]. The observation in $^{120}$Sn [31] of a width value similar to the ground state one in nuclei at $T = 1$ MeV cast further doubts on the validity of the calculations in the low temperature region. A similar result was obtained in the systematic study of angular momentum gated GDR width of $^{119}$Sb in a temperature region between 0.9 and 1.4 MeV using fusion reactions with alpha particles [71]. The LAMBDA spectrometer (see Fig. 1) was used to measure the high energy gamma rays. The GDR width values measured for $T < 1$ MeV are consistent with the ground state value of $^{119}$Sb while a smooth increase is observed at higher temperature. The overall trend of the GDR width as function of the temperature up to $T = 3$ MeV for nuclei of mass $A = 118$–120 is shown in Fig. 9b [72]. Red full circles correspond to $^{119}$Sb data while other points are from previously existing systematics. The observed trend is in complete contrast to the TSFM which predicts a gradual increase of the GDR width from the ground state value, as shown by the dashed line. Similar considerations hold for $^{63}$Cu data shown in Fig. 9a [61,73] and for $^{201}$Tl plus $^{208}$Pb data shown in Fig. 9c [72]. These results called for a new interpretation of the GDR width suppression with respect to the TSFM predictions. The proposed explanation is that the GDR vibration induces a quadrupole moment causing the nuclear shape to fluctuate even at zero temperature. If these fluctuations are comparable or larger in size than the thermally induced ones no effect can be observed in the spectral shape. This argument leads to the existence of a temperature, called critical temperature ($T_c$), representing the threshold temperature above which thermal fluctuation effects can be observed on the GDR width [72]. This idea of a $T_c$ somehow mirrors the interpretation used to explain the nuclear deformation effects on the GDR width. In fact, in the TSFM, an increase of GDR width is observed only when the equilibrium deformation $\beta_{eq}$ becomes larger than thermal shape fluctuation contribution. The model postulating the existence of a critical temperature, called Critical Temperature included Fluctuation Model, is purely empirical but allows to describe the data trend in different mass regions as shown in Fig. 9 [72]. It is interesting to note that the critical temperature decreases with the increase of the nuclear mass and shows a linear behavior with $1/A$ which can be described through the relation $T_c = 0.7 + 37.5/A$ [72]. Recently, new data taken on $^{81}$Rb at $E^* = 54$ MeV were found in agreement with CTFM predictions [74].

The experimental evidence and theoretical framework discussed in this paragraph show that both angular momentum and temperature are effective in driving the nucleus towards more deformed or elongated shapes. They influence the GDR width which becomes progressively broader with increasing excitation energy. However recent data taken at temperature below $T < 1.5$ MeV showed some limitations of the TSFM in describing the width trend raising new questions on the basic understanding of the width increase at low $T$. The existence of a critical temperature above which the GDR width starts to increase was postulated by some authors. The observed discrepancy between data and TSFM predictions at very low $T$ was somehow reduced including the effect of

pairing field fluctuations which improved significantly the agreement between data and calculations in different mass regions [10,75,76].

## 5 The GDR behaviour up to 4 MeV temperature

Populating hot nuclei at progressively higher excitation energies led to the appearance of new phenomena in the study of the GDR properties. In particular, the smooth increase of the width, explained in terms of temperature induced and spin driven effects was observed to undergo an abrupt change after the study of the reaction $^{40}$Ar + $^{70}$Ge at 10$A$ MeV [77]. In this experiment hot nuclei of $^{110}$Sn at $E^* = 230$ MeV were populated through fusion reactions. Complete fusion events corresponding to a full linear momentum transfer from the projectile to the compound system were selected in $\Delta E$-ToF matrix measured with PPACs and retained in the analysis. Gamma-ray energy spectra showed a clear bump associated to the GDR decay and, at higher energies, the typical tail due to the bremsstrahlung contribution originating from nucleon-nucleon collisions in the first stage of the reaction. The statistical model calculations allowed for a reproduction of the gamma spectra assuming a Lorentzian shape for the GDR with 100% of the EWSR, a centroid energy of 16 MeV and a width of 13 MeV constant over the whole decay path. A constant level density parameter $a = A/8$ was used in the calculations. Different attempts were also made to reproduce the spectra varying the level density parameter, the width and GDR strength. This procedure allowed for an estimate of the error bar in the GDR parameters of about 1 MeV both for the centroid and the width. The value of 13 MeV extracted for the width, shown in Fig. 10 as a star symbol, is similar to the one previously measured at 130 MeV for nuclei in the same mass region. Such a result suggested, for the first time, a possible onset of a width saturation effect above 130 MeV. The width was expected to increase due to thermal fluctuations and spin effects. The observation of a width saturation at 230 MeV excitation energy suggested the main contribution to the width increase was not linked to the temperature but to the angular momentum. In fact, in fusion evaporation reactions, the transferred angular momentum increases with beam energy up to the maximum value a nucleus can sustain without fissioning. In nuclei of mass $A \sim 110$ such a value is reached around $E^* \sim 100$ MeV suggesting that at higher excitation energies the width should not depend on spin effects. The difference of about 2 MeV between data and thermal fluctuation model predictions suggested also the presence of other temperature dependent couplings, besides thermal fluctuations, which can contribute to the GDR width.

Further evidence for a saturation of the GDR width was observed in the study of the reaction $^{136}$Xe + $^{48}$Ti at 18.5$A$ MeV [78]. In this case hot nuclei were populated through

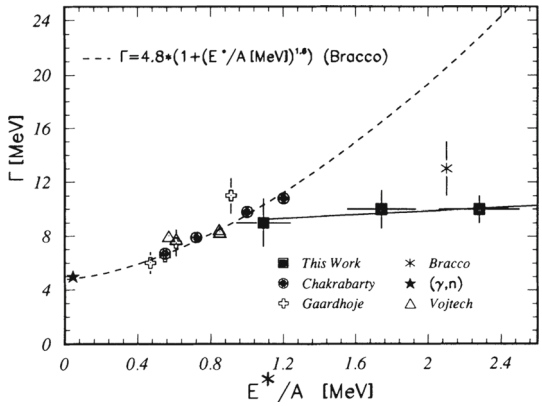


**Fig. 10** The existing systematics on the GDR built on Sn isotopes are shown as a function of $E^*/A$. Full squares represent the data from Enders et al. [78] showing the width saturation. The star symbol shows the width value measured in the work of Bracco et al. [77]. The solid line is a fit to the Enders data while the dashed one shows a fit to the Sn data (from Ref. [78])

deep inelastic collisions. From the full kinematical reconstruction of the heavy fragments, using mass and momentum conservation, the total excitation energy of the hot nuclei was inferred. Pre-equilibrium particle emission was taken into account applying a correction based on the systematics of linear momentum transfer [79]. Gamma-rays were detected in concidence with binary events using three arrays of $BaF_2$ scintillators located at 50°, 90° and 150°. In order to investigate the excitation energy dependence of the GDR width, gamma-ray energy spectra were built selecting three different regions of excitation energy. They were reproduced with statistical model calculations assuming two contributions, one from the projectile and the other from the target, the dominant contribution being the one associated to the heavier Xe-like fragment. The GDR width was found to be approximately constant, around a value of 10 MeV, at all excitation energies, and seemed to be insensitive to the particular choice of the level density adopted in the statistical calculation. The results of this work are shown in Fig. 10 together with the existing systematics built on Sn isotopes. Hofmann et al. [80] investigated the GDR properties in the same mass region using $^{16}$O beams of 200 and 280 MeV impinging on $^{118}$Sn target. Assuming complete fusion between the reaction partners, it was possible to populate hot nuclei at excitation energies of 165 and 235 MeV respectively [80]. Gamma-ray energy spectra measured in the study of the reaction at 200 MeV beam energy were reproduced with statistical model calculations using 100% of the EWSR, a centroid energy $E_{GDR}$ = 15.2 MeV and a width of 10.5 MeV. Similar values were extracted in the analysis of the data at 280 MeV indicating an agreement, within the error bar, with Enders' results on the width saturation. Different values of the level density parameter were adopted in the calculations to evaluate

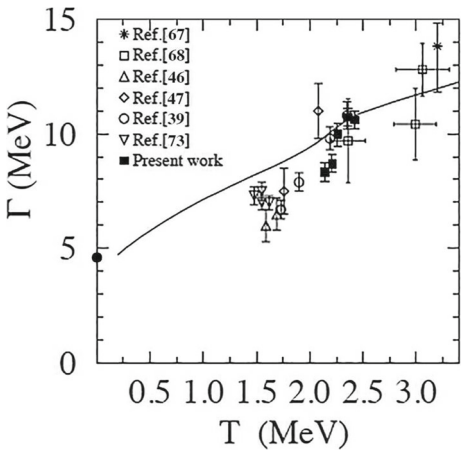


**Fig. 11** GDR width as a function of the nuclear temperature (adapted from Ref. [52]). Data from Ref. [52] are shown as full squares while the existing systematics are shown as open symbols. Data from Refs. [77] and [78] are corrected for pre-equilibrium emission

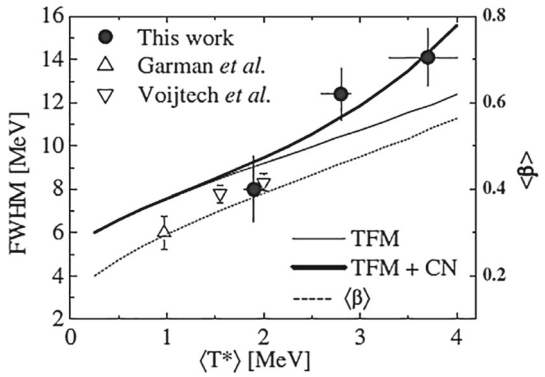


**Fig. 12** GDR width as a function of the temperature calculated as a weighted average over approximately 50% of the total yield (from Ref. [50]). Data from the reaction $^{64}$Ni + $^{68}$Zn at $E_{\text{beam}}$ = 300, 400 and 500 MeV are shown as full symbols. Other data are from Garman et al. [85] and from Voijtech et al. [84]. The thin line shows the predictions of the thermal shape fluctuation calculation while the thick one includes the effect of compound nucleus lifetime as predicted by Chomaz [69]

their influence on the GDR shape parameters. An error bar of 0.5 MeV on the GDR shape parameters was deduced from the comparison with data. The authors made also statistical model calculations including corrections for incomplete momentum transfer which reduce the excitation energy by about 10%. The new calculations led to a variation of about 5% in the width values which did not affect the conclusions concerning the width saturation [80].

More recently a study of the light charged particle energy spectra emitted in the reaction $^{18}$O + $^{100}$Mo at 200 MeV highlighted some limits in the determination of excitation energy in fusion reactions using the systematics of momentum transfer [81]. The study of the light charged particle energy spectra showed the presence of a contribution arising from pre-equilibrium emission which lowers the excitation energy of the system. In order to disentangle the contributions of the different emitting sources, proton and alpha particle energy spectra measured in coincidence with gamma-rays and evaporation residues were reproduced through a fitting procedure assuming the isotropic emission from two moving sources, one associated to the compound nucleus and the other with pre-equilibrium emission. The energy distribution of the emitted particles was parametrized, in the source rest frame, according to a surface-type Maxwellian distribution. The amount of energy removed by the pre-equilibrium emission was evaluated from the multiplicities and the average temperatures of the intermediate source extracted from the fit of the particle energy spectra. Neutron pre-equilibrium emission was estimated from a Fermi jet model calculation. It was found that pre-equilibrium emission removed, on average, about 20% of the compound nucleus excitation energy and three mass units relative to the complete fusion values while the linear momentum transfer was reduced only by 8%. Such an approach was used by the same authors to investigate the GDR properties in the Sn mass region using the same reaction spanning the excitation energy range where the GDR width was observed to saturate. At variance with previous works the values of the GDR width, shown as full symbols in Fig. 11, were observed to increase from 8.3 to 10.6 MeV for temperatures ranging from 2.14 to 2.42 MeV [52]. Besides, in the same work, a simple relation used to estimate the excitation energy loss as a function of projectile energy per nucleon was deduced from the pre-equilibrium data [52]. Such a relation was then applied to the existing data taken using beam energies above 10$A$ MeV. This approach produced a general lowering of the excitation energy estimates compared to the original works. The re-analysis of the gamma spectra using the new values of excitation energy led to an increase of the extracted GDR widths whose values, after the re-analysis, increases up to $T \sim 3.2$ MeV in the Sn mass region as shown in Fig. 11 [52,82]. The comparison of the width data extracted from about $T = 1.4$ MeV to 3.2 MeV [47,55,56,77,78,83] with the calculations based on the adiabatic thermal shape fluctuation model shown in the same figure as full line, supported this conclusion.

The reinterpretation of the old data raised important questions concerning the GDR width behaviour at $T > 2$ MeV. The new picture of a GDR width increasing with temperature motivated a new investigation using data without preequilibrium contribution whose subtraction is model dependent. A symmetric reaction $^{64}$Ni + $^{68}$Zn at $E_{\text{beam}}$ = 300, 400 and 500 MeV was chosen to populate nuclei at excitation energies ranging from 100 to 200 MeV [50]. Light charged particles were measured in coincidence with gamma-rays and evaporation residues. In particular, the study of the proton and alpha particle energy spectra showed that their emission originated from a single thermalized source associated to the compound

system therefore excluding any sizeable contribution from pre-equilibrium emission. Gamma-ray energy spectra were reproduced using statistical model calculations performed assuming a GDR centroid energy of 14 MeV, 100% of the EWSR and a width increasing from $8 \pm 1.5$ to $14.1 \pm 1.3$ MeV for systems corresponding to $E^* = 100$ and 200 MeV respectively. The temperature of the compound system was calculated as a weighted average over approximately 50% of the total yield, from initial conditions along the decay process, where at each step the weight is represented by the gamma yield in the GDR region [51]. The average temperatures deduced for the three reactions are 1.9, 2.8 and 3.7 MeV. The measured width values are shown in Fig. 12 as full symbols [50]. The other data in the same figure are taken from Refs. [84] and [85] and show the systematics at lower temperatures corresponding to reactions leading to fully thermalized compound nuclei. In this work, the GDR width in nuclei of mass region $A = 110$–$132$ is observed to increase with temperature up to about 3.7 MeV. The increase cannot be fully described in terms of TSFM whose prediction is shown by the thin line in Fig. 12. In order to reproduce the data trend up to the highest temperatures one needs to include within TSFM the contribution of nuclear lifetime [50,69].

The experimental findings up to 200 MeV excitation energy depict a scenario where the strength of the GDR retains 100% of the EWSR and the width progressively increases due both to temperature and spin effect, the latter mainly playing a role above 35–40$\hbar$ depending on the nuclear mass. There is no evidence of a saturation of the width, the one observed in the past experiments being mainly related to an underestimation of the pre-equilibrium emission which lowers the compound nucleus excitation energy more than evaluated from the linear momentum transfer measurements.

However, a recent measurement on the $^{88}$Mo nucleus raised new questions concerning a possible saturation of GDR width [46]. In the experiment hot nuclei were populated at $E^* = 124$ and 261 MeV using the reaction $^{48}$Ti + $^{40}$Ca at 300 and 600 MeV. The analysis of the light charged particle energy spectra didn't show any clear evidence of pre-equilibrium emission and therefore the statistical model analysis of the gamma spectra was performed assuming for the excitation energy the value reached in complete fusion reactions. The comparison of the gamma-ray energy spectra with statistical model calculations led to the extraction of a width value almost constant at the two excitation energies suggesting a saturation of the width at variance with what observed in $^{132}$Ce nuclei. Results are shown in Fig. 13 as full symbols together with the existing systematics on Mo nuclei [36,86,87]. The shaded area in the figure indicates the predictions of the Kusnezov parametrization for spin ranging from 10 to 30 $\hbar$ [61], the spin interval where the different data were extracted. Data are well described up to 2 MeV temperature while above such a value the calculations overshoot the data.

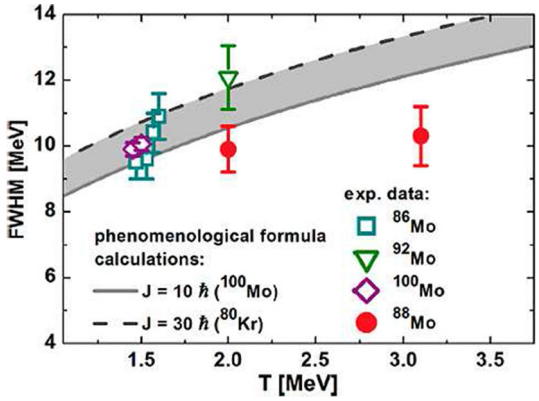


**Fig. 13** Measured GDR widths as a function of nuclear temperature for different Mo isotopes (from Ref. [46]). Full symbols represent data on $^{88}$Mo measured by Ciemala et al. [46], open squares show data on $^{86}$Mo [36], open triangles show data on $^{92}$Mo [87] and open diamonds show data on $^{100}$Mo [86]. The shaded region shows the predictions of the phenomenological formula of Kusnezov et al. for the GDR width evolution with temperature in Mo nuclei, in a spin range from 10 to 30$\hbar$ [61]

The observed saturation of the width has been explained by the authors as due to the higher rotational frequency in $^{88}$Mo nuclei compared to $^{132}$Ce due to a lower moment of inertia [46]. This idea lead to the conclusion that the GDR width in $^{88}$Mo is mainly governed by rotation induced deformation phenomena and not so much affected by temperature effects. Besides, to reproduce the data at 261 MeV the GDR strength was reduced to 80% of EWSR, a value which might support the hypothesis of the onset of another phenomenon, subject of the next section, the GDR quenching at high excitation energies.

## 6 GDR quenching

The study of the GDR populated in hot nuclei at very high excitation energies (or temperatures) allows one to probe the collective behaviour in nuclei in extreme conditions up to its disappearance. In fact, the GDR gamma-ray emission is sufficiently fast to compete with other decay modes with a sizeable branching ratio and therefore to probe the characteristics of the nuclear system prevailing at that time. However, the compound nucleus lifetime progressively decreases with excitation energy and the time needed to equilibrate collective degrees of freedom could become comparable or even longer than the nuclear lifetime. This would strongly affect the measured GDR strength distribution which reflects the competition between the different time scales associated to the population and decay of the GDR on one side and the compound nuclei lifetime on the other. Therefore, the study of the GDR properties at high excitation energies represents an important testing ground to investigate the limits of valid-

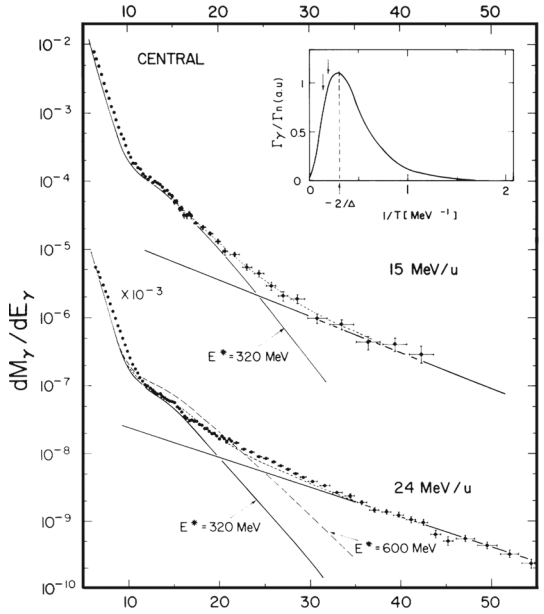


**Fig. 14** Gamma-ray spectra measured in coincidence with evaporation residues in the reactions $^{40}$Ar + $^{70}$Ge at 15 and 24$A$ MeV beam energies (from Ref. [88]). Full line shows the statistical model calculation performed at $E^* = 320$ while the dashed line represents a calculation at $E^* = 600$, the excitation energy of the hot fused system populated in the reaction at 24$A$ MeV. The sum spectra, for each reaction, built using statistical (at $E^* = 320$ MeV) plus bremsstrahlung contribution are shown as dotted lines

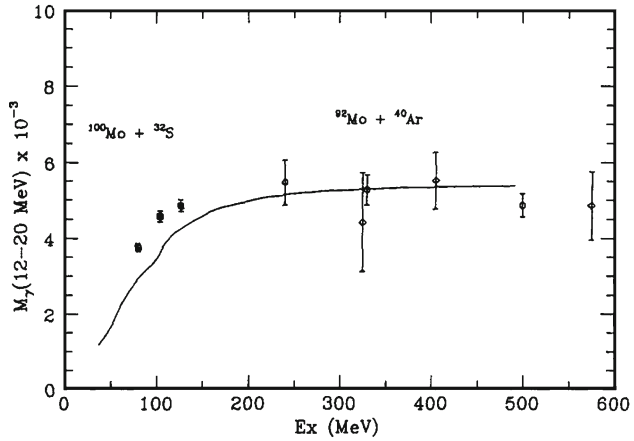


**Fig. 15** Trend of the GDR gamma multiplicity obtained integrating the region $12 \leq E_{GDR} \leq 20$ MeV of the spectra from the reactions $^{40}$Ar + $^{92}$Mo at 21$A$ MeV and 26$A$ MeV after bremsstrahlung subtraction and from reactions $^{32}$S + $^{100}$Mo at beam energies of 150, 180 and 210 MeV. The full line shows the trend of the GDR gamma multiplicity as deduced from statistical model calculations performed at different excitation energies using a width dependent on the excitation energy of the system (from Ref. [91])

ity of the statistical compound nucleus theories in describing the decay properties of nuclei.

### 6.1 Earlier experiments

The experimental investigation at high excitation energies was mainly focused in the Sn mass region where broad systematics were collected. The first pioneering work on this topic was performed by Gaardhøje et al. who studied the evolution of the GDR decay as a function of the excitation energy using the reaction $^{40}$Ar + $^{70}$Ge at 15 and 24$A$ MeV beam energies [88]. Hot nuclei formed in incomplete fusion reactions were populated at average excitation energies of $E^* = 320$ MeV and $E^* = 600$ MeV. The gamma-ray spectrum at $E^* = 320$ MeV, shown in Fig. 14, retains the main GDR features observed in experiments at lower excitation energy, and was reproduced assuming a Lorentzian shape for the GDR with 100% of the EWSR, a centroid energy of $E_{GDR} = 15.5$ MeV and a width $\Gamma = 15$ MeV. Such a result indicated for the first time the persistence of the collective motion up to these excitation energies. In constrast, at $E^* = 600$ MeV a sizeable strength reduction was observed. The statistical model calculation performed at 600 MeV and shown in Fig. 14 as a dashed line, strongly overshoots the data at 24$A$ MeV. The gamma-ray spectrum was reproduced assuming the same value of excitation energy used to reproduce the one at 15$A$ MeV and is shown in Fig. 14 as a full line. Such a result could not be explained in the framework of a statistical model scenario due to the higher number of decay steps available for the GDR gamma emission to compete with particle decay. Part of the difference can be ascribed to an improper estimate of pre-equilibrium particle emission which was done applying a correction to the complete fusion estimate through linear momentum transfer systematics. However, even taking into account the effects related to a variation in the level density parameter (in the original paper $a = A/8$ was assumed) the discrepancy would be reduced but the general conclusions remain the same. This observation suggested, for the first time, the existence of a limiting excitation energy for the collective motion at about 320 MeV.

In order to search for new evidence of the quenching phenomenon, new studies on the GDR behaviour at high excitation energies were carried out at the RIKEN Ring Cyclotron using the reactions $^{40}$Ar + $^{92}$Mo at 21$A$ MeV and 26$A$ MeV [89]. High energy gamma-rays were measured in coincidence with fusion-like residues. Events were selected applying gates on different recoil velocities which correspond, in a simple massive transfer scenario, to different average excitation energies. The average excitation energy for each velocity window was estimated assuming that the whole target merges with a fraction of the projectile mass, the remaning part moving in forward direction with its initial velocity. A wide window in excitation energy, from 265 to 610 MeV, was populated in the reactions. The average masses of the compound systems ranged from 109 to 132. Neutron spectra, measured in coincidence with recoils of different velocity, were analysed assuming the emission from two Maxwellian

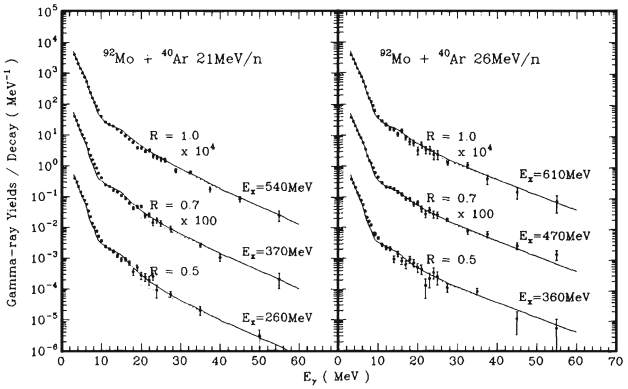


**Fig. 16** The left panel shows gamma-ray spectra for the reaction $^{40}$Ar + $^{92}$Mo at 21$A$ MeV measured in coincidence with evaporation residues. Three velocity bins were applied to the residue velocity corresponding to average excitation energies of 260, 370 and 540 MeV. The right panel shows spectra for the reaction $^{40}$Ar + $^{92}$Mo at 26$A$ MeV built using the same approach. In this case the values of average excitation energies are 360, 470 and 610 MeV. Full lines show the sum of the statistical model calculations performed assuming a width progressively increasing with excitation energy and the fit of bremsstrahlung contributions (from Ref. [89])

sources, one associated to the pre-equilibrium and the other to the equilibrated system. Data were reproduced through a fitting procedure which allowed the extraction of the main features of both pre-equilibrium and thermal sources. Neutron multiplicities and temperatures emitted from the thermal source were observed to increase with excitation energy. Statistical model calculations performed with CASCADE nicely reproduced the measured values of the neutron multiplicity and temperature assuming a level density parameter ranging from $A/8$ to $A/9$ supporting the scenario of a statistical emission from a thermalized source formed at progressively higher excitation energy [89,90].

Gamma-ray spectra were extracted for both reactions and all the velocity bins. The GDR gamma-ray yield, integrated in the region $12 \leq E_{\mathrm{GDR}} \leq 20$ MeV after bremsstrahlung subtraction, was observed to be almost constant, within the error bar, in the whole region above 250 MeV excitation energy as shown in Fig. 15, in agreement with the Gaardhøje et al. results [89,91]. Standard statistical model calculations assuming for the GDR a centroid energy $E_{\mathrm{GDR}}$ = 15.5 MeV, a width $\Gamma_{\mathrm{GDR}} = 20$ MeV and a strength equal to 100% of the EWSR failed to reproduce the data showing a strong overprediction of the yield in the GDR region.

In order to reproduce the spectra the authors proposed two approaches, either to quench the gamma emission above a critical excitation energy or to include in the statistical code an energy dependence of the GDR width [89]. The first approach lead to the conclusion of the existence of a limiting excitation energy or temperature above which the GDR suddenly disappears. The second approach was based on the observation that the GDR width increases with excitation energy at lower temperatures. A phenomenological energy dependence of the width, which was allowed to vary along the decay process, was introduced in CASCADE to reproduce the spectra without any reduction of the EWSR strength. This was a really new approach since, traditionally, each single calculation was performed assuming a constant width along the decay process. The best data reproduction, shown in Fig. 16 as a full line, was obtained assuming an excitation energy dependence given by the relation $\Gamma_{\mathrm{GDR}} = 4.8 + 0.035E + 1.6 \cdot 10^{-8} E^4$ for both reactions. This formula suggests that, at variance with the apparent width which increases gently with excitation energy, the width increases very rapidly being about 20 MeV at $E^* = 160$ MeV and 40 MeV at $E^* = 205$ MeV. Such an increase induces a spread of the GDR strength in a progressively broader region leading to a quenching of the gamma-ray yield in the GDR peak region. The calculations allow a reasonable reproduction of the saturation effect of the gamma multiplicity above about 250 MeV excitation energy as shown by the full line in Fig. 15. This approach leads to the conclusion that the GDR disappearance is connected to a progressive broadening of the resonance. The author defined, somehow arbitrarily, a limiting excitation energy for the GDR as the value corresponding to a GDR width equal to 30 MeV. Using the width parametrization adopted to reproduce the spectra in CASCADE, the deduced limiting excitation energy is 180 MeV.

The explanation of the saturation of the GDR gamma multiplicity in terms of a strongly increasing width found a significant theoretical support in a series of works in which the GDR disappearance was explained in terms of a width increase with excitation energy (or temperature) [92–94] even if the energy dependence of the width predicted by the theory was milder then the one used to fit the data. However, this was not the only approach used by theoreticians to explain the GDR quenching phenomenon. Other ideas based on the the competition between the nuclear lifetime and the time needed for the system to equilibrate collective degrees of freedom were also proposed [95,96]. A re-analysis of the data was undertaken by the RIKEN group including the effect of equilbration time and the results showed that it was possible to obtain a good fit of the data assuming for the width an energy dependence similar to the one found by Chakrabarty at lower excitation energies [91,97] and therefore in agreement with the theoretical approach proposed by Smerzi et al. [92,93]. The net effect of this re-analysis of the data is that the limiting excitation energy for the collective motion would rise to about $E^* = 300$ MeV.

The different approaches will be shortly reviewed in the following paragraph and then we will proceed in describing the more recent experimental results on the GDR quenching following a historical approach.

### 6.2 Theoretical models

Theoretical interpretations of the GDR quenching effect point to two main effects to explain the data, either a rapid increase of the width or a real yield suppression. The idea of a rapid increase of the GDR width was explored in a series of works where the interplay between one- and two-body dissipation was investigated through a semiclassical approach based on the Vlasov equation with a collisional relaxation time [92–94]. The study of the temperature dependence of the escape width $\Gamma^{\uparrow}$ and of the spreading width $\Gamma^{\downarrow}$ contributions to total GDR width showed that while the escape width is of the order of few hundred keV the spreading width strongly increases due to 2-body collisions. This effect becomes progressively more important because of the Pauli blocking suppression with increasing temperature. The model predicts an increase of the width with excitation energy similar to the trend described by the Chakrabarty et al. parametrization [47] for the width found at lower excitation energies [93,94]. At about $E^* = 230$ MeV the calculations predict a GDR spreading width of the order of the resonance energy. Therefore the contribution to the gamma-ray spectrum of hot nuclei populated at these or even higher energies is spread out over a very broad energy range. The results suggest that the GDR progressively disappears due to a broadening of the resonance with excitation energy.

A different interpretation, again based on the width increase, was proposed by Chomaz to explain the GDR yield saturation [69]. The key issue of this approach is that the total GDR width should include the contributions coming from the evaporation width $\Gamma_{ev}$ of the compound nucleus states. According to the Heisenberg uncertainty principle, each nuclear level involved in the GDR gamma decay has an intrinsic width, associated to its finite lifetime $\tau$ due to particle evaporation. This implies that transition energies between nuclear levels cannot be determined better than twice the intrinsic width. This indetermination affects the total width of the resonance but not the centroid energy. Assuming for each nuclear level an intrinsic width equal to the evaporation width of the compound nucleus $\Gamma_{ev}$ the total GDR width then becomes:

$$\Gamma_{GDR} = \Gamma^{\downarrow} + 2\Gamma_{ev} \tag{6}$$

The added contribution induces a rapid increase of the GDR width which starts to be significant in the region of $E^* \approx$ 150–200 MeV.

The strong dependence of the width on the excitation energy predicted by both models could explain the disappearance of the GDR at high excitation energies but the gamma-ray energy spectral shape is expected to show an increase of the yield in the region above the resonance due to the spread of the yield connected to the width increase. This will be the critical region to investigate when data will be compared to statistical model calculations including the model prescriptions described above.

GDR yield suppression models instead explain the GDR quenching as an effect due to the competition between the equilibration times associated to the different degrees of freedom, in particular the collective ones, and nuclear lifetime. With increasing nuclear excitation energy, the assumption of the statistical model of a full thermalization of collective degrees of freedom could not always be fulfilled in the hot system. In fact the nuclear lifetime would reduce significantly and could become comparable or shorter than the time needed to develop a collective oscillation [95]. In this case, the system would decay by particle evaporation before being able to develop a collective oscillation which would appear when the system has already cooled down part of its initial excitation. The effect is governed by the relative sizes of the evaporative width $\Gamma_{ev}$ and the GDR spreading width $\Gamma^{\downarrow}$ [96]. Bortignon and coworkers proposed that the compound nucleus states can exist in two different classes, with or without the GDR. Assuming that GDR states are not populated at the beginning of the reaction, the excitation energy at which the spreading width and evaporative width are comparable defines a critical temperature for the existence of collective motion [96]. Above this temperature, in fact, the compound nucleus will evaporate particles, reducing its excitation energy, before the GDR can develop. Such an approach gives a possible explanation of the observed saturation of the GDR yield. The model predicts a quenching factor given by the relation [96]:

$$F = \Gamma^{\downarrow}/(\Gamma^{\downarrow} + \Gamma_{ev}) \tag{7}$$

where $\Gamma^{\downarrow}$ is the GDR width on the ground state and $\Gamma_{ev}$ is the evaporative width which increases with excitation energy.

The effects of equilibration time for the different degrees of freedom was re-investigated by Snover [82]. Starting from the expression of the probability of the equilibration of a collective vibration, which depends on the spreading width of the resonance and the time elapsed in the decay process, he deduced a GDR suppression factor which, for the $n$th decay step, is given by the relation:

$$F_n \sim 1 - exp\left(-\Gamma^{\downarrow}\sum_{i=1}^{n}\Gamma_{ev}(i)^{-1}\right) \tag{8}$$

where $\sum_{i=1}^{n}\Gamma_{ev}(i)^{-1}$ is related to the elapsed time in the decay process expressed in terms of widths, $t_{ev}(i) = \hbar/\Gamma_{ev}(i)$ being the mean life time for the $i$th decay step and $\Gamma_{ev}(i)$ the evaporative width. The predicted inhibition factor attains, at the first step, a value similar to the one predicted by Eq. 7. However during the decay process, as the excitation energy decreases, it approaches unity more rapidly becoming negligible already around 300 MeV due to the effect of cumulative lifetime while the factor given by Eq. 7 still predicts

a sizeable suppression in the same excitation energy range. Snover concluded that the non-equilibration of the collective motion is too small an effect to explain the GDR saturation at high excitation energies.

A more detailed description of the different models can be found in a previous review paper [9] and references therein.

### 6.3 Further evidence of yield saturation

After the evidence of a GDR quenching found in the study of the reaction $^{40}$Ar + $^{92}$Mo at 21$A$ MeV and 26$A$ MeV, further studies were undertaken by the RIKEN group at lower excitation energies to map the evolution of the GDR properties in a region where the quenching is expected to set in. Hot nuclei of $^{132}$Ce were populated at excitation energies of 80, 103 and 125 MeV using the reaction $^{32}$S + $^{100}$Mo at incident energies of 150, 180 and 210 MeV. Fusion events were selected, gating on high gamma-ray multiplicity events and data analysis was performed accordingly. The analysis of the gamma-ray energy spectra showed that the GDR multiplicity, integrated in the region $12 \leq E_{\mathrm{GDR}} \leq 20$ MeV, was increasing with excitation energy. However the increase between 103 and 125 was about one half of that between 80 and 103 indicating an onset of saturation already around 120 MeV. The spectra could be reproduced using the same parametrization of the width adopted at higher excitation energies. This allowed to reasonably describe the whole set of data as a function excitation energy from 80 to 500 MeV, as shown by the full line in Fig. 15.

The results of Gaardhøje and Kasagi clearly showed the existence of the GDR quenching in hot nuclei at high excitation energies. However, the different hypotheses adopted in the data analysis led the authors to different conclusions on both the value of the limiting excitation energy for the collective motion and the mechanism responsible for the quenching phenomenon. In order to find an answer to the open questions concerning the reasons of the GDR quenching at high excitation energy a series of experiments was performed using the MEDEA detector [27] at GANIL and more recently at the LNS-Catania. The GANIL experiments were performed using $^{36}$Ar beams at 27$A$ and 37$A$ MeV impinging respectively on $^{90}$Zr and $^{98}$Mo targets. Hot nuclei populated in the reactions were characterized through a complementary analysis of the recoil velocities and the study of light charged particle spectra [26,98]. Time of flight spectra were divided in three velocity bins corresponding to different average excitation energies and average masses and the data analysis was performed accordingly. In the case of 27$A$ MeV data the excitation energy was estimated comparing the values deduced from the massive transfer approach with the excitation energy values deduced from temperatures extracted from the fit of proton energy spectra, corrected to infer the initial temperature of the compound system. Deduced excitation energy values range from 350 to 550 MeV while initial masses range from $A = 108$ to $A = 120$ [22,98].

Data at 37$A$ MeV were treated in a similar way, but the excitation energies were estimated from the residue velocities using the massive transfer model whose results were corrected for pre-equilibrium light charged particle emission which was evaluated through a fit of all light charged particle energy spectra [26]. Estimates for neutron emission were also included in the correction. This approach was made possible due to to an improved timing of the 37$A$ beam compared to 27$A$ data set which led to a better isotopic separation of $Z = 1$ particles. The calculated amount of pre-equilibrium emission was then subtracted from the $E^*$ values calculated with the massive transfer model to infer the initial excitation energy and mass of the system for each velocity bin. Such correction lead to an improvement in the evaluation of the excitation energies in the 37$A$ MeV data which are, for this reason, lower than the 27$A$ MEDEA data and also lower than RIKEN data, both not corrected for pre-equilibrium emission. This data treatment led to average values of excitation energy of 300, 350 and 430 MeV for the hot systems populated in the three different velocity bins [26,28].

Gamma-ray spectra were extracted for all velocity bins and integrated in the region $12 \leq E_{\mathrm{GDR}} \leq 20$ MeV after bremsstrahlung subtraction for both reactions. The GDR gamma-ray yield extracted in the analysis of 27$A$ MeV data, was observed to be constant within the error bar in the whole excitation energy region investigated. Similar considerations hold for the 37$A$ MeV data even if a slightly smaller average GDR yield was measured.

The analysis of the 27$A$ MeV gamma-ray spectra was undertaken through a comparison with standard statistical model calculations assuming a single Lorentzian shape for the GDR with a strength equal to 100% of the EWSR, a centroid energy parametrized by $E_{\mathrm{GDR}} = 76/A^{1/3}$ and a constant width $\Gamma = 12$ MeV. A level density parameter dependent on the temperature according to the Ormand parametrization [99] was adopted in the calculation. Such a choice was motivated by the strong temperature dependence of the level density parameter which is a crucial ingredient in the statistical model calculation and by the large excitation energy range explored in the full data set which cannot be properly described by a single level density value. Calculations were performed assuming an initial spin of 50$\hbar$, a value close to the maximum angular momentum that a Sn nucleus can sustain before fission. Fig. 17 shows the comparison between bremsstrahlung subtracted gamma-ray energy spectra measured for the 350 MeV and 500 MeV excitation energy and the associated standard Cascade calculations shown as dashed lines. The low energy part of the spectra is reasonably well reproduced while, in the GDR region, the calculations strongly overshoot the data, the difference being more pronounced with increasing the excitation energy of the system.

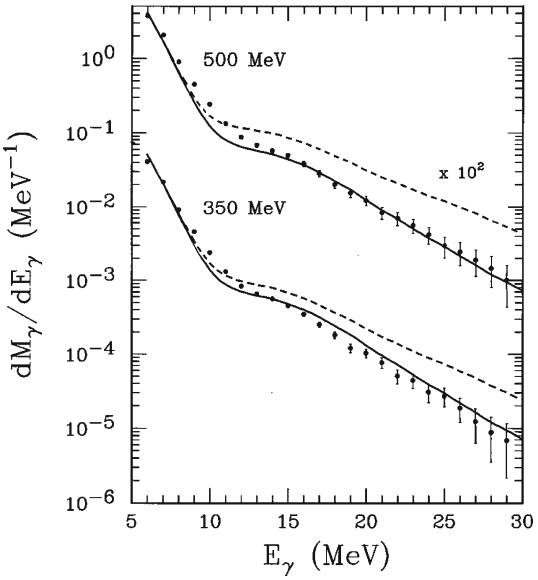


**Fig. 17** Gamma-ray spectra after bremsstrahlung subtraction measured in the reaction $^{36}$Ar + $^{90}$Zr at 27$A$ MeV (adapted from Ref. [22]) in coincidence with evaporation residues of 350 MeV and 500 MeV average excitation energies. Dashed lines represent the standard statistical model calculations performed with CASCADE using a GDR width $\Gamma = 12$ MeV and a centroid energy parametrized according to the relation $E_{\mathrm{GDR}} = 76/A^{1/3}$. Full lines corresponds to calculations using a sharp cutoff of the gamma emission at 250 MeV excitation energy

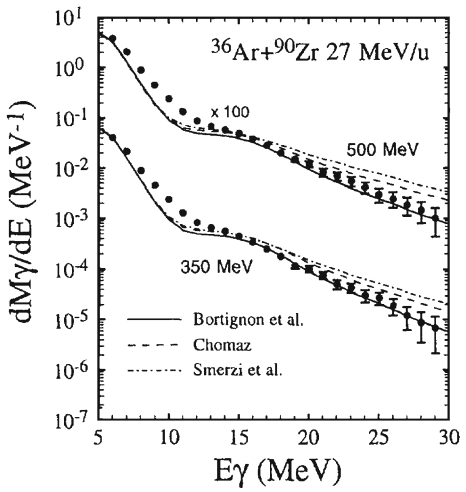


**Fig. 18** Gamma-ray spectra after bremsstrahlung subtraction measured in coincidence with evaporation residues populated at 350 MeV and 500 MeV excitation energy using the reaction $^{36}$Ar + $^{90}$Zr at 27$A$ MeV (from Ref. [100]). Dashed lines represent the predictions of statistical model calculations performed including model prescriptions of Chomaz [69]. Full lines corresponds to calculations including model prescriptions of Bortignon et al. [96] while dot-dashed lines show the results of Smerzi et al. model [92]

This result is clear evidence of a GDR quenching at these very high excitation energies. The simplest way to reproduce the data was to introduce in the statistical model calculations a sharp suppression of the gamma emission above a given excitation energy, the so called cut-off energy. In the analysis of the 27$A$ MeV data the authors reproduced the spectra extracted at all the excitation energies using the same cut-off value of 250 MeV. Using this approach data were well reproduced except in the region between 8 and 12 MeV where the calculations underestimate the measured gamma yield as shown by the full lines in Fig. 17 [22]. Some possible explanations of this extra strength were proposed by the authors but the reasons, being associated either to nuclear structure effects, to the reaction dynamics or to a simplified parametrization of the sharp cut-off, remain hitherto unexplained.

Data were also compared to statistical model calculations including the different theoretical prescriptions of the GDR disappearance at high excitation energies, previously described, to find an answer concerning the mechanism leading to the GDR quenching. The results of the different calculations for 350 MeV and 500 MeV excitation energy are compared to the data in Fig. 18 [100]. Solid line corresponds to Bortignon et al. [96] predictions, dot-dashed line to Smerzi et al. [92] predictions while the dashed line shows the Chomaz one [69]. Both models describing the GDR quenching in terms of a continuosly increasing width lead to a decrease of the yield in the region of the GDR centroid but fail to reproduce the spectra above about 20 MeV where the calculations overestimate the yield, the prediction being even larger than the standard statistical calculation. The reason of this effect can be found in the statistical dipole emission rate formula where two ingredients contribute to induce a shift of the yield at higher energies rather than a quenching: the level density ratio, being roughly proportional to $\exp(-E_\gamma/T)$, tends, with increasing temperature, to increase the $\gamma$ multiplicity at higher energies by decreasing the slope of the spectrum and the $E_\gamma^2$ factor which multiplies the Lorentzian representing the GDR strength function which shifts the $\gamma$ yield to higher energies when the GDR width increases. Such considerations hold for all models including a width increase in the calculation. Such a result is in clear contradiction with RIKEN results which interpreted the effect as due to a progressive GDR width increase. One possible explanation of these contradictory results could be attributed to the limited statistics of the RIKEN data in the bremsstrahlung region which prevented a proper determination of the bremsstrahlung contribution. This affected the high energy part of the statistical spectrum precluding a correct comparison of the data with statistical model calculations in this energy domain.

Conversely, the comparison of the data with the smooth cut-off prescription based on Bortignon et al. model gives a reasonable reproduction of the data above about 13 MeV while between 8 and 12 MeV the calculations underestimate the gamma yield similarly to what was previously observed using the sharp cut-off approach. The results of the MEDEA

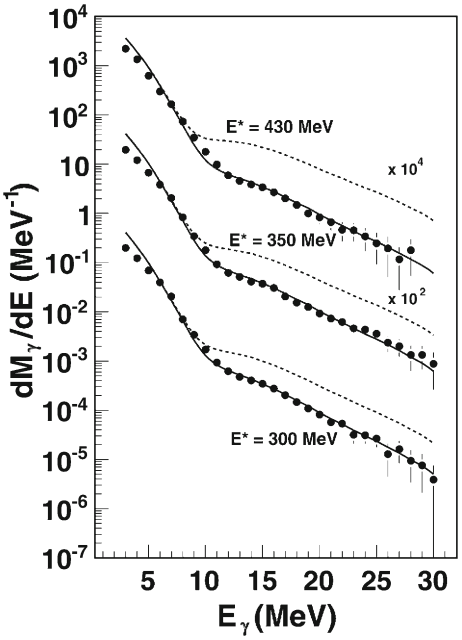


**Fig. 19** Gamma-ray spectra after bremsstrahlung subtraction measured in coincidence with evaporation residues of average excitation energies $E^* = 300$, 350 and 430 MeV populated in the study of the reaction $^{36}$Ar + $^{98}$Mo at 37$A$ MeV. Standard statistical model calculations are shown as dashed lines while full lines correspond to statistical calculations which include a sharp cutoff of the gamma emission at 220 MeV for $E^* = 300$ and 430 MeV while a slightly higher value of 230 MeV was used for systems at $E^* = 350$ MeV (from Ref. [28])

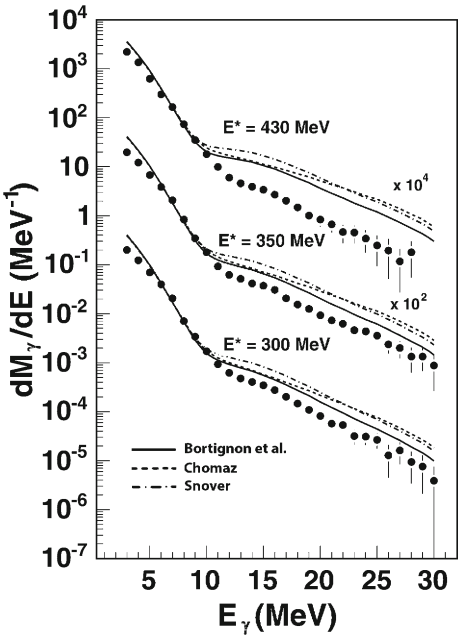


**Fig. 20** Gamma-ray spectra after bremsstrahlung subtraction measured in coincidence with evaporation residues of average excitation energies $E^* = 300$, 350 and 430 MeV populated in the study of the reaction $^{36}$Ar + $^{98}$Mo at 37$A$ MeV. Statistical model calculations performed using the smooth cutoff prescription of Bortignon et al. are shown as full lines, calculations using the Snover smooth cutoff are shown as dot-dashed lines while dashed lines show the predictions of the width increasing model of Chomaz

experiment at 27$A$ MeV clearly depict a scenario in which the GDR gamma-ray saturation is consistent with a quenching of the GDR strength around approximately 250 MeV excitation energy. This led the authors to conclude that $E^*/A \sim 2.3$ to 2.5 MeV represents a limit for the existence of the dipole vibration for $A \sim 110$ nuclei [98].

The study of the reaction $^{36}$Ar + $^{98}$Mo at 37$A$ MeV was undertaken in a similar fashion. Gamma-ray energy spectra measured in coincidence with evaporation residues of different excitation energy were compared with statistical model calculations performed with DCASCADE (a new version of the CASCADE code) assuming for the GDR a resonance energy $E_{GDR} = 15$ MeV, a width $\Gamma_{GDR} = 13$ MeV and a strength $S_{GDR} = 100\%$ of the EWSR. A level density parameter dependent on the temperature of the system was adopted following the parametrization suggested by Ormand et al. [99] similarly to what previously done for the 27$A$ MeV data. The results of the calculations folded with the detector response are shown in Fig. 19 as dashed lines. The comparison shows that the calculations strongly over-predict the data in the GDR region at all excitation energies while the low energy region is still reasonably well reproduced. The effect increases with the excitation energy of the system. Following the approach already used during the analysis of the 27$A$ MeV data, in the attempt to reproduce the spectra in a simple way, the authors included in the calculations a sharp cut-off of the gamma emission above a given excitation energy. The best agreement with the data was obtained using a cut-off of the gamma emission at 220 MeV for 300 and 430 MeV excitation energies while a slightly higher value of 230 MeV gave the best fit to the data taken at $E^* = 350$ MeV [28]. The same values of the GDR parameters and level density parametrization used in the standard approach were adopted in the calculations. The agreement between calculations, shown as full lines in Fig. 19, and data is remarkably good over more than five orders of magnitude in cross section and down to 3 MeV energy. The extracted cutoff values, while being slightly lower than the value of 250 MeV deduced in the analysis of 27$A$ MeV data confirms the existence of a limiting excitation energy for the collective motion that for nuclei of mass $A \sim 108$, corresponds to $E^*/A \sim 2.1$ MeV [28]. The small differences observed in the cut-off values deduced in the analysis of 27$A$ and 37$A$ MeV could be ascribed to the different version of the code used to reproduce the gamma-ray spectra.

The data were also compared to different model prescriptions which were implemented by the authors in DCASCADE. The results of Bortignon et al. [96], Chomaz [69] and Snover [82] model predictions were folded with the detector response and are shown for comparison in Fig. 20. While the

low energy part of the gamma-ray spectra is well reproduced in yield and shape in all calculations, none of the models is able to reproduce the GDR region. The Snover smooth cut-off produces a very soft quenching, the Chomaz approach yields a spectral shape not able to reproduce the data while the Bortignon cutoff is the one which is the closest to the data, especially at 300 MeV excitation energy. The discrepancy between data and predictions increases with increasing excitation energy for all the models suggesting some limitations in describing the possible mechanism that suppresses the collective vibration.

The results of the MEDEA experiments performed at GANIL clearly depicted a scenario where the observed GDR $\gamma$-ray saturation is consistent with a sudden disappearance of the GDR strength in a region around 220–250 MeV (using the sharp cut-off approach). The results could not be explained in terms of width increasing models, differently from what previously inferred from the RIKEN data [89], because the main effect of such approach is to induce a shift of the yield towards high energies, an effect not observed in both experiments at 27$A$ and 37$A$ MeV.

If these results added an important piece of information in the comprehension of the GDR quenching, a few important elements of the scenario were still missing. In particular, the region where the quenching appears was still unknown due to a lack of experimental data below the cut-off energy value as well as the mechanism that induces the suppression of the collective motion. In order to find an answer to these open questions an experimental campaign was undertaken at the Laboratori Nazionali del Sud (LNS) Catania using $^{116}$Sn beams at 17$A$ and 23$A$ MeV impinging on both $^{12}$C and $^{24}$Mg targets [28,29]. Such a choice allowed the authors to map the evolution of the GDR properties in a wide excitation energy range, from values where the GDR retains its typical features to values where the quenching is clearly evident. Light charged particles and gamma-rays were detected with MEDEA in coincidence with evaporation residues focused by the magnetic field of the Superconducting Solenoid SOLE on the focal plane detector MACISTE [28,101]. Inverse kinematic reactions were used to better match the Solenoid acceptance. For each reaction, events belonging to a single narrow velocity window centered around the center of mass velocity, were retained in the data analysis and the study of light charged particles and gamma-rays was performed accordingly.

As in the analysis of the 37$A$ MeV experiment the characterization of the hot nuclei was performed combining the information deduced from the study of the ToF spectra of the evaporation residues with the analysis of the light charged particle energy spectra to estimate the amount of pre-equilibrium emission. The values of excitation energy deduced from such a procedure range from $E^* = 150$ MeV for the reaction $^{116}$Sn + $^{12}$C at 17$A$ MeV to $E^* = 330$ MeV for the reaction $^{116}$Sn + $^{24}$Mg at 23$A$ MeV. In order to have a better control on the reaction mechanism and on the estimated values of average excitation energy, mass and charge of the hot nuclei populated in reactions, the $Z$ distributions of evaporation residues were measured for the reactions $^{116}$Sn + $^{24}$Mg at 17$A$ and 23$A$ MeV [29]. The comparison with GEMINI++ [44] simulations, properly filtered with the spectrometer acceptance, assuming as input a decaying system whose main features are those deduced from the analysis described above, shows a reasonably good reproduction of the data in terms of centroid and width as shown in Fig. 6. This result supported the scenario of incomplete fusion and, at the same time, strengthened the deduced average values of excitation energy, mass and charge of the hot system populated in the reactions.

The evolution of the GDR properties as a function of the excitation energy was investigated through a comparison of the gamma-ray spectra, bremmstrahlung subtracted, with standard statistical model calculations performed with the code DCASCADE, modified to calculate the GDR strength at each step of the decay process. A level density parameter dependent on the temperature of the system was adopted according to the Ormand et al. parametrization. Shell effects were taken into account using the Reisdorf formalism based on the Ignatyuk espression for the level density [42,43]. The best fit to the spectra at $E^* = 150$ MeV and 190 MeV was obtained assuming for the strength 100% of the EWSR, a centroid energy $E_{\mathrm{GDR}} = 14.3 \pm 0.3$ MeV, and a width $\Gamma_{\mathrm{GDR}}$ increasing from $11.0 \pm 0.8$ MeV to $12.5 \pm 1.0$ MeV [28]. A very good data reproduction was obtained, as shown in Fig. 21a. At $E^* = 270$ and 330 MeV it was no longer possible to fit the data with a reasonable set of parameters. Calculations were performed assuming a centroid energy $E_{\mathrm{GDR}} = 14$ MeV and a width $\Gamma_{\mathrm{GDR}} = 13$ MeV. Both calculations overshoot the data, the discrepancy being more pronounced at $E^* = 330$ MeV as shown in Fig. 21a. This result clearly shows that the onset of the GDR quenching appears above 200 MeV excitation energy in nuclei of this mass region [29]. In order to better judge the quality of the fit to the data, the linearized spectra $\mathrm{M}_{\gamma-\mathrm{exp}}/\mathrm{M}_{\gamma-\mathrm{CASCADE}} \times F(E_\gamma)$ are plotted in Fig. 21b and compared to $F(E_\gamma)$ where $F(E_\gamma)$ is the Lorentzian function used in DCASCADE to describe the GDR decay, arbitrarily normalized to one.

Following the approach already used to fit the data at 27$A$ and 37$A$ MeV, the spectra at 270 MeV and 330 MeV were reproduced assuming a sharp cut-off of the gamma emission above a given excitation energy. The best fit to the data was obtained using a cut-off value of 230 MeV for $E^* = 270$ MeV and of 240 MeV for $E^* = 330$ MeV, values consistent with the results extracted at higher excitation energies in nuclei of mass $A \sim 110$. Both spectra and calculations are shown in Fig. 22a [29]. The results would indicate a sudden disappearance of the dipole vibration in nuclei of mass

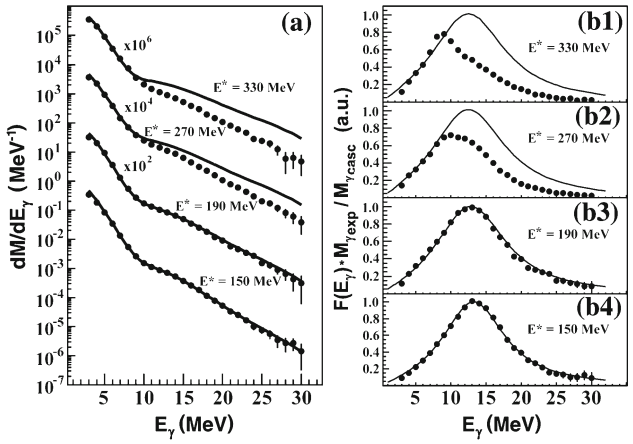


**Fig. 21** **a** Gamma-ray spectra, bremsstrahlung subtracted, measured in the study of the reactions $^{116}$Sn + $^{12}$C and $^{116}$Sn + $^{24}$Mg both at 17$A$ and 23$A$ MeV. Full lines show the results of standard statistical model calculations. **b** Linearized spectra (see text) compared with the Lorentzian function used, in statistical model calculations, to describe GDR decay (solid line) (adapted from Ref. [28])

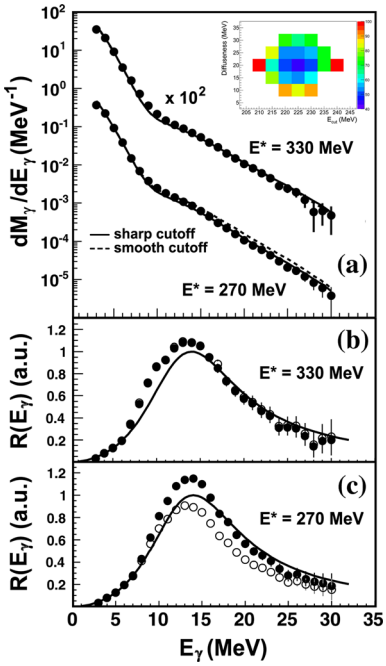


**Fig. 22** **a** Comparison of the gamma-ray energy spectra, bremsstrahlung subtracted, with statistical model calculations, performed using a sharp (full line) and smooth (dashed line) cutoff of the gamma emission parametrized according to a Fermi function. **b** Comparison of the linearized gamma-ray spectra, $R(E_\gamma) = M_{\gamma-\mathrm{exp}}/M_{\gamma-\mathrm{CASCADE}}$ x $F(E_\gamma)$, measured at $E^* = 330$ MeV with the Lorentzian function used, in statistical model calculations, to describe the GDR decay arbitrarily normalized to one. Open symbols correspond to smooth cutoff calculations while full symbols correspond to the sharp cutoff ones. A sharp cutoff value of 240 MeV was used in the calculation. **c** Same as **b** for spectra measured at $E^* = 270$ MeV. A sharp cutoff value of 230 MeV was used in this case in the calculation to better reproduce the data (from Ref. [29])

$A = 124$–$132$ for excitation energies around $E^*/A \sim 1.7$ to 1.8 MeV. However, as already pointed out, the inclusion of a sharp cut-off of the gamma emission in the statistical model is an oversimplified approach as one expects a progressive GDR disappearance as a function of the excitation energy. In order to investigate the shape of the cutoff the authors implemented in DCASCADE a GDR quenching factor, excitation energy dependent, parametrized according to a Fermi function. Different calculations varying the Fermi function parameters were carried out. The best agreement was found assuming a progressive suppression of the gamma emission above 200 MeV excitation energy using a value of $E_{\mathrm{cut}}$, the energy value at which the Fermi function reduces to one half, equal to 225 MeV and value of 20 MeV for the diffuseness [29]. Statistical model calculations performed using these values of the parameters are shown in Fig. 22a as dashed lines. As it can observed from the figure, the results are close to the one obtained using a sharp cutoff approach, especially at $E^* = 330$, but in that approach two different values of the cutoff were used to reproduce the data. In panel b of the same figure, the linearized spectra measured at $E^* = 330$ using the two cutoff shapes are compared to $F(E_\gamma)$ the Lorentzian function used in DCASCADE to describe the GDR decay, arbitrarily normalized to one. Panel c shows the same comparison for the spectra measured at $E^* = 270$. This approach allows to better evaluate the small differences in the calculations which are somehow masked when data are shown in log scale as in panel a. The results clearly indicated, for the first time, that the GDR quenching is a rather sharp phenomenon, the GDR fully disappearing in about 100 MeV excitation energy.

Calculations including different theoretical model prescriptions were also performed by the authors. The results showed, even in this excitation energy range, that none of the models can fully describe the whole data set nor the sudden disappearance of the GDR observed experimentally as a function of the excitation energy. The best agreement was obtained using the approach of Bortignon et al. which however overpredicts the gamma yield in the GDR region at $E^* = 270$ and $E^* = 330$ MeV while suggesting a rise of the quenching phenomenon already at $E^* = 190$ MeV where the data lay above the calculation [102].

In order to quantify the progressive GDR quenching as a function of the excitation energy of the system, gamma-ray energy spectra and statistical model calculations were integrated in the region between 12 and 20 MeV where the GDR yield is mainly concentrated. Fig. 23a shows the trend of the experimental data as a function of excitation energy per nucleon. Full circles represent the gamma-ray multiplicities extracted from data at 17$A$ and 23$A$ MeV while full triangles show the multiplicities measured in the study of the reaction $^{36}$Ar + $^{98}$Mo at 37$A$ MeV. The gamma-ray multiplicity is

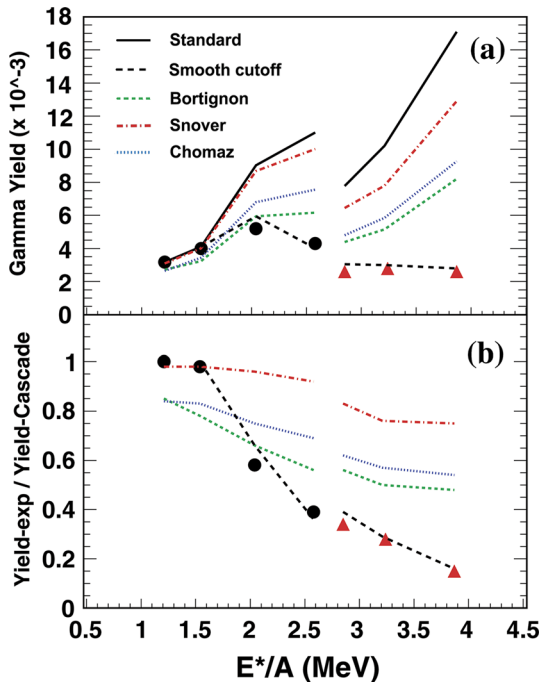


**Fig. 23** **a** GDR gamma-ray multiplicity integrated in the region 12–20 MeV as a function of excitation energy per nucleon. Full circles represent the data measured in the study of the reactions $^{116}$Sn + $^{12}$C and $^{116}$Sn + $^{24}$Mg both at 17$A$ MeV and 23$A$ MeV. Full triangles represent the multiplicities extracted in the study of the reaction $^{36}$Ar + $^{98}$Mo at 37$A$ MeV. Solid lines show the trend of the multiplicity predicted by the standard statistical model obtained integrating the spectra in the region 12–20 MeV. Green dashed, blue dotted and red-dot-dashed lines indicate the trend of the Bortignon, Chomaz and Snover model predictions respectively. Long dashed lines show the multiplicity trend deduced from calculations including a smooth cutoff as described in the text. **b** Full symbols show the ratio of the experimental gamma multiplicity to standard statistical model calculations. The different lines represent the ratio of the multiplicity trend extracted from calculations including model predictions to standard statistical model calculations. Same colors and line types as in **a** are used (from Ref. [102])

observed to increase as a function of $E^*/A$ up to about 2 MeV. Above such a value a saturation effect is observed for nuclei with similar masses. Gamma-ray yield extracted in the study of the reaction $^{36}$Ar + $^{98}$Mo at 37$A$ MeV is rather constant, within the error bar, as a function of $E^*/A$ but the measured values are lower than those extracted at lower excitation energies [28]. Such a result can be explained in terms of a combined effect of the quenching and the different mass and charge of the nuclei populated in the two data sets which affect the value of $NZ/A$ factor in the formula of the decay width for statistical E1 gamma-decay. The comparison of the experimental data with the results of the standard statistical model calculations, connected by a solid line, shows that the absolute values of the multiplicity and the trend are well reproduced up to about $E^*/A \sim 1.6$ MeV. Above such a value the data progressively start to fall below the calculations, the effect being more pronounced when the comparison is extended to 37$A$ MeV data. In the same figure the trends of the Bortignon et al., Chomaz and Snover model predictions are presented respectively as dashed, dotted and dot-dashed lines. Such a quantitive comparison shows in better detail the differences already observed in the comparison of the spectral shapes predicted by different quenching models with data. Only the Bortignon et al. model predictions lay close to the data up to about $E^*/A \simeq 2$ MeV. A good reproduction of the full data set is obtained using the smooth cutoff approach, shown in Fig. 23a as a long dashed line and parametrized according to the Fermi function previously described in the text where the same values of $E_{\rm cut}$ and diffuseness were used in all the calculations [102].

In the attempt to remove the $NZ/A$ dependence and investigate the evolution of the GDR quenching as a function of excitation energy the ratio between experimental and calculated yield was built for each excitation energy per nucleon assuming as a reference the standard statistical model calculations. The results shown in Fig. 23b as full circles and full triangles clearly indicate a smooth decrease of the ratio, arising above 1.5 MeV and suggesting that a GDR quenching sets in around 1.8 MeV excitation energy [102]. The same ratio was also built for the different model predictions. The smooth cutoff approach allows to nicely reproduce the abrupt onset of the quenching of the collective vibration observed in the experimental data up to about $E^*/A = 4$ MeV. The reasons for such rather sharp phenomenon remain hitherto unexplained. The search for the mechanism that suppresses the collective motion has to be found in the competition between collective motion and particle decay.

### 6.4 Mass dependence of the GDR quenching

The bulk of existing data on the evolution of the GDR properties at very high excitation energies is concentrated in nuclei of mass $A = 105$–$132$. However, a few experiments investigated the GDR properties in other mass regions to search for evidence of a GDR quenching. The first attempt was undertaken by the RIKEN group who studied the reactions $^{40}$Ar + Ni, $^{36}$Ar + $^{92}$Mo and $^{40}$Ar + $^{122}$Sn at 26$A$ MeV [91]. Hot nuclei with average excitation energies of about 450, 500 and 500 MeV and average masses $A = 72$, 105 and 130 respectively were populated in the reactions. These estimates are based on a massive transfer model approach and do not take properly into account the pre-equilibrium emission which is underestimated. Therefore they should be considered as upper limits to the real excitation energy values of the hot decaying systems. Same considerations hold for the values of the average masses extracted from the data analysis. To reproduce the gamma-ray spectra using a fixed width it was necessary to introduce a sharp cutoff of the gamma emission above a given value of excitation energy, determined through a best fit procedure, which was interpreted as the limiting

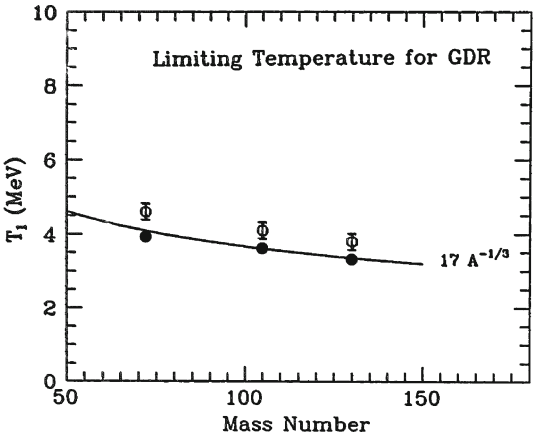


**Fig. 24** Trend of the limiting temperature for the existence of the GDR as a function of the system mass as deduced by the RIKEN group. Open circles are obtained from a comparison of data with statistical model calculations assuming a fixed width and a sharp cutoff of the gamma emission. Full circles are deduced from a comparison with statistical model calculations performed assuming a width dependent on excitation energy. In this case the limiting excitation energy or temperature was defined as the value above which the GDR width becomes larger than 30 MeV. Solid line shows the $17{\cdot}A^{-1/3}$ dependence as discussed in the text (from Ref. [91])

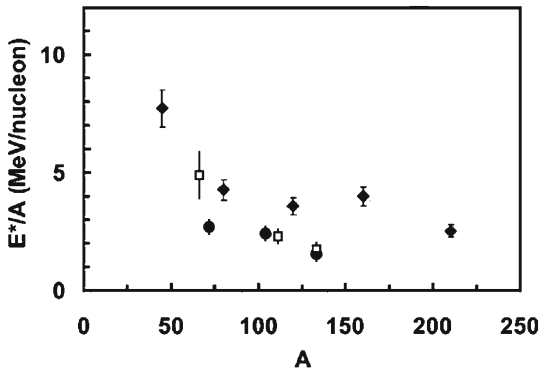


**Fig. 25** Values of excitation energies per nucleon at which the plateau in the nuclear caloric curve sets in, shown as full diamonds, are compared to the limiting excitation energy for the collective motion as a function of the system mass. MEDEA and TRASMA data are shown as open squares while RIKEN data are shown as full circles

excitation energy for the collective motion. The excitation energy values deduced from the analysis of the gamma-ray spectra are $E^* = 190 \pm 20$, $230 \pm 30$, and $230 \pm 30$ MeV for $^{40}$Ar + Ni, $^{36}$Ar + $^{92}$Mo and $^{40}$Ar + $^{122}$Sn respectively. For each system the corresponding limiting temperature was calculated assuming $E^* = A/8 \cdot T^2$. The deduced values are $4.6 \pm 0.2$, $4.1 \pm 0.2$, $3.8 \pm 0.2$ MeV. A decreasing trend as a function of the mass number is observed as shown in Fig. 24 [91]. When the excitation energy dependence of the width is included in the calculations, a critical excitation energy for the GDR disappearance cannot be defined since the disappearance is no more sudden but progressive due to the width increase. The authors, somehow arbitrarily, defined a limiting excitation energy or temperature as the value above which the GDR width becomes broader than 30 MeV. Using such a definition, the values of the limiting excitation energy for the GDR are 140 MeV for $^{40}$Ar + Ni reaction and 180 MeV for the two other reactions. The corresponding temperatures, range from 3.9 to 3.3 MeV as shown in Fig. 24. Data can be reasonably well described by a $17 \cdot A^{-1/3}$ dependence as shown by the full line in the same figure.

A further evidence for the GDR quenching was observed in the mass region $A \sim 60$ to 70 studying the reactions $^{40}$Ca + $^{48}$Ca and $^{40}$Ca + $^{46}$Ti at 25$A$ MeV with the TRASMA detector [103] at the LNS Catania. Hot nuclei were populated through incomplete fusion reactions at $E^* = 355$ MeV and 335 MeV using $^{48}$Ca and $^{46}$Ti targets respectively [104,105]. Gamma-rays were detected in coincidence with evaporation residues. The comparison of the gamma-ray spectra with statistical model calculations performed assuming for the GDR a centroid energy $E_{\mathrm{GDR}} = 16.8$ MeV, a width $\Gamma = 15$ MeV and a strength equal to 100% of EWSR provided clear evidence for a GDR quenching at these excitation energies. In order to reproduce the spectra in a simple way the authors introduced a sharp cut-off of the gamma emission in the statistical model calculations. The best agreement with the data on $^{48}$Ca was obtained assuming a cut-off energy equal to 260 MeV keeping the same values of GDR parameters used in the standard calculation. A smaller value of 200 MeV was instead used to reproduce the spectra on the $^{46}$Ti target. Taking into account the average masses of the two systems, values of $E_{\mathrm{cut-off}}/A \simeq 4.7$ MeV and 3.8 MeV [104,105] for $^{48}$Ca and $^{46}$Ti targets respectively were deduced as a limiting excitation energy for the collective vibration. More refined calculations including the prescriptions of different smooth cut-offs were also performed. A good description of the data was obtained for both reactions adopting the smooth cut-off suggested by Bortignon et al. [96]. Using this approach a cut-off energy of the gamma emission was defined as the excitation energy value which leads to a quenching factor $\Gamma^{\downarrow}/(\Gamma^{\downarrow} + \Gamma_{ev}) = 1/2$. Cut-off energy values of about $5.4 \pm 0.5$ $A$ MeV and $4.7 \pm 0.9$ $A$ MeV were extracted from the analysis of $^{48}$Ca and $^{46}$Ti targets [105]. These values are slightly higher than those extracted using the sharp cut-off approximation and higher than the values measured by the RIKEN group in a similar mass region.

The results obtained from the analysis of the gamma-ray spectra in different mass regions provided evidence for a mass dependence of the limiting excitation energy (or temperature) for the existence of the GDR. The disappearance of the collective motion has been interpreted by some theoreticians as one of the possible signatures for a phase transitions

in nuclei [106,107]. From this point of view, probing the limits of the collective motion in nuclei represents a complementary approach to extract information on the liquid-gas phase transition which has been investigated using different experimental probes and theoretical approaches. Among these, the study of the caloric curve, the dependence of the nuclear temperature on its excitation energy, has provided evidence of a trend reminiscent of the liquid water heating to the boiling point, the plateau region being interpreted as the liquid-gas phase transition in nuclear matter [39]. One interesting feature of these studies is the mass dependence of the plateau temperature which decreases as a function of nuclear mass. This affects the excitation energy value where the plateau region sets in which decreases from about 8 MeV for nuclei with mass $A = 30$–$60$ to about 3 MeV in nuclei of mass $A = 180$–$240$ [39]. The values of the excitation energy per nucleon where the transition appears, in five different mass regions, are shown in Fig. 25 as full diamonds. In the same figure the values of the limiting excitation energy for the collective motion collected in different experiments with MEDEA and TRASMA are shown as open squares while the RIKEN data are shown as full circles. The comparison shows interesting similarities both in the trend and in the absolute values. In particular, the limiting excitation energies for the GDR are close to the energy values where the liquid–gas phase transition sets in suggesting the occurrence of a transition from order to chaos in nuclei for excitation energies close to the values where the liquid–gas phase transition was claimed to be present. A discrepancy in the limiting exctation energy values for the collective motion appears in the mass region $A = 50$–$70$ where data extracted with the TRASMA detector are much higher than the RIKEN result. The origin of the discrepancy could be, at least partly, related to an improper evaluation of the pre-equilibrium emission which would lower the average mass of the emitting system increasing the estimate of the limiting excitation energy per nucleon for the existence of the GDR. The discrepancy could be further reduced if the sharp cutoff value deduced in the analysis of TRASMA data is used in the systematics instead of the smooth cut-off one [105].

However, the observed similarities do not exclude different explanations concerning the reasons of the measured trend. In fact, the cutoff energy values extracted in all the experiments except the RIKEN data for mass $A = 72$ range between 220 and 250 MeV. At these excitation energies nuclear lifetimes could become comparable or even shorter than the time needed for the system to equilibrate collective degrees of freedom leading to a decay of the system before the development of the collective motion. The GDR spectral shape at high excitation energy would simply reflect the competition between the different time scales without any link with a phase transition. New GDR data collected in heavier nuclei of mass around $A = 180$–$200$ could be the key to disentangle between the different interpretations.

## 7 Conclusions and perspectives

The gamma-decay of the Giant Dipole Resonance represents a fundamental probe to explore basic nuclear properties at finite temperatures and angular momentum. A broad range of topics including shape fluctuactions and shape evolution of hot rotating nuclei, isospin symmetry, Jacobi transitions, fission timescales, loss of collectivy and also phase transitions have been addressed through its investigation. Over the past thirty years important steps forward in the comprehension of the main GDR properties has been carried out both from the theoretical and experimental points of view. A broad systematics on the evolution of the main GDR features as a function of temperature and angular momentum has been built for nuclei in different mass regions, using mainly inelastic scattering and/or fusion reactions. Data collected from different experiments clearly showed that the GDR centroid energy exhibits no significant dependence as a function of the excitation energy (or temperature) while the width was found to progressively increase as a function of angular momentum and temperature up to about $T = 4$ MeV. Theoretical appproaches mainly based on the TSFM are able to describe most of the data on the width evolution as a function of spin while its temperature dependence is not fully reproduced. In particular, recent measurements have shown that the GDR width doesn't increase from its ground state value up to about $T = 1$ MeV, the exact value being inversely proportional to the nuclear mass. This behaviour cannot be explained in the framework of the TSFM and a possible explanation has been suggested. However, the recent implementation of pairing fluctuations inside the model improved the agreement between data and theory at low T. Further measurements are needed to confirm the present results as well as some theoretical work to describe in a more consistent way the whole set of data available.

Moving to higher temperatures, the systematics of the width increase above $T \sim 2$ MeV and up to 4 MeV can be only reproduced by the TSFM including an additional contribution arising from the compound nucleus lifetime. In this range of temperatures, in particular above $T \sim 2.5$ MeV the earlier measurements indicated a saturation of the width which was recently explained, after a re-analysis of the data, as due to an improper evaluation of the pre-equilibrum emission which lowers the excitation energy of the system affecting the data interpretation. New data, using reactions without pre-equilibrium emission whose subtraction is model dependent, clearly showed a progressive increase of the width up to $T \sim 4$ MeV in nuclei of mass $A \sim 130$. However, new

evidence for a saturation of the GDR width in $^{88}$Mo at $T = 3$ MeV was recently published showing that there is presently no clear scenario. In order to get a deeper understanding of the trend of the GDR width in this range of temperatures further experiments addressing this issue would be important.

In order to disentangle temperature from spin induced effects, the evolution of the GDR width as a function of spin was investigated selecting a narrow range of temperatures of the hot system populated in the reaction. The angular momentum information was typically obtained from a low energy $\gamma$-ray multiplicity filter. Data taken in nuclei with $T < 1.5$–1.8 MeV have shown a weak dependence on the angular momentum of the system for low J values while above about $J = 35$–$50\hbar$, depending on the mass of the system, a progressive increase of the width has been observed. In heavy nuclei there is no clear signature of a dependence of the GDR width on the angular momentum. The reason can be found in the mechanism driving the deformation, the rotational frequency. For a given J the rotational frequency decreases as a function of the nuclear mass reducing the effect in heavier nuclei.

Above $E^* = 230$–250 MeV much evidence of a saturation of the GDR gamma-ray yield were found at variance with statistical model calculations which predict a progressive increase with excitation energy. Earlier conclusions concerning the main mechanism leading to the saturation were somehow controversial due to an improper evaluation of the pre-equilibrium particle emission which led to a wrong estimate of the excitation energy and mass of the hot system. This affected the results of the statistical model calculations which use these quantities as input parameters to reproduce the statistical decay of the hot system populated in the reaction. In some cases also the limited statistics in the high energy component of the gamma-ray spectrum may have affected the proper determination of the bremsstrahlung contribution precluding a correct comparison of the spectral shape with statistical model calculations in the region above the resonance energy.

More recently, experiments performed using detector arrays with high detection efficiency for $\gamma$-rays and light charged particles allowed for an improved control on the reaction dynamics, in particular on the pre-equilibrium emission which provided a better characterization of the hot decaying nuclei. A few experiments were carried out with the aim to explore the excitation energy region where the quenching was expected to set in. A detailed mapping of the progressive quenching was undertaken measuring the GDR properties from a region where the GDR still retains 100% of the EWSR to a region where the quenching is clearly observed. A coherent scenario emerged where the $\gamma$-ray energy spectra measured in nuclei with mass $A \sim 120$–132 can be reasonably well reproduced assuming a sudden drop of the GDR strength at excitation energies $E^* = 230$–250 MeV. The comparison of the data with model predictions showed that the spectral shape is not compatible with a continuous increase of the width as predicted in some theoretical papers while it is better described by models interpreting the drop in strength as due to a competition between the equilibration of collective motion and particle decay. However none of the models can reproduce the full set of data up to $E^* = 430$ MeV due to a surprisingly sudden onset of the GDR quenching not predicted by any of the existing models. The results clearly indicated, for the first time, that the GDR fully disappears in a range of about 100 MeV excitation energy.

Whether this abrupt disappearance of the resonance can be related to a nuclear phase transition remains an open question. In order to investigate this possibility, it would be important to extend the existing systematics to higher mass ($A \sim 180$–200) nuclei. Finally, the quenching phenomenon deserves a better understanding also from the theoretical point of view with an improvement of the existing models or the development of new approaches which could better describe the sharp trend observed, its mass dependence and eventually its possible link with a liquid-gas phase transition.

**Acknowledgements** D. Santonocito thanks the Université Paris-Sud for the invitation as invited professor during which part of the paper was written.

**Data Availability Statement** This manuscript has no associated data or the data will not be deposited. [Authors' comment: This is a review paper which shows data already published.]



## References

1. M.N. Harakeh, A. Van der Woude, *Giant Resonances: Fundamental High-Frequency Modes of Nuclear Excitation* (Oxford Science Publications, Oxford, 2001)
2. P .F. Bortignon, A. Bracco, R. Broglia, *Giant Resonances: Nuclear Structure at Finite Temperature* (Harwood Academic Publishers, Reading, 1998)
3. G.C. Baldwin, G.S. Klaiber, Phys. Rev. **71**, 3 (1947)
4. D. M. Brink, Ph.D thesis, University of Oxford, Oxford (1955)
5. P. Axel, Phys. Rev. **126**, 671 (1962)
6. A. Buda, J.C. Bacelar, A. Balanda, H. van der Ploeg, Z. Sujkowski, A. van der Woude, Nucl. Phys. **A553**, 509c (1993)

7. K.A. Snover, Ann. Rev. Nucl. Part. Sci. **36**, 545 (1986)
8. J.J. Gaardhøje, Ann. Rev. Nucl. Part. Sci. **42**, 483 (1992)
9. D. Santonocito, Y. Blumenfeld, Eur. Phys. J **A30**, 183 (2006)
10. D.R. Chakrabarty, N Dinh Dang, V.M. Datar, Eur. Phys. J **A52**, 143 (2016)
11. P. Paul, T. Thoennessen, Ann. Rev. Nucl. Part. Sci. **44**, 65 (1994)
12. I. Diószegi, N.P. Shaw, A. Bracco, F. Camera, S. Tettoni, M. Mattiuzzi, P. Paul, Phys. Rev. C **63**, 014611 (2001)
13. S. Ceruti, F. Camera, A. Bracco, R. Avigo, G. Benzoni, N. Blasi, G. Bocchi, S. Bottoni, S. Brambilla, F.C.L. Crespi, A. Giaz, S. Leoni, A. Mentana, B. Million, A.I. Morales, R. Nicolini, L. Pellegri, A. Pullia, S. Riboldi, O. Wieland, B. Birkenbach, D. Bazzacco, M. Ciemala, P. Désesquelles, J. Eberth, E. Farnea, A. Görgen, A. Gottardo, H. Hess, D.S. Judson, A. Jungclaus, M. Kmiecik, W. Korten, A. Maj, R. Menegazzo, D. Mengoni, C. Michelagnoli, V. Modamio, D. Montanari, S. Myalski, D. Napoli, B. Quintana, P. Reiter, F. Recchia, D. Rosso, E. Sahin, M.D. Salsac, P.-A. Söderström, O. Stezowski, Ch. Theisen, C. Ur, J.J. Valiente-Dobón, M. Zieblinski, Phys. Rev. Lett. **115**, 222502 (2015)
14. A. Bracco, F. Camera, Phys. Scr. **91**, 083002 (2016)
15. A. Bracco, F. Camera, F.C.L. Crespi, B. Million, O. Wieland, Eur. Phys. J **A55**, 233 (2019)
16. A. Maj, M. Kmiecik, A. Bracco, F. Camera, P. Bednarczyk, B. Herskind, S. Brambilla, G. Benzoni, M. Brekiesz, D. Curien, G. De Angelis, E. Farnea, J. Grebosz, M. Kicinska-Habior, S. Leoni, W. Meczynski, B. Million, D.R. Napoli, J. Nyberg, C.M. Petrache, J. Styczen, 0. Wieland, M. Zieblinski, K. Zuber, N. Dubray, J. Dudek, K. Pomorski, Nucl. Phys. A **731**, 319 (2004)
17. K. Mazurek, J. Dudek, A. Maj, D. Rouve, Phys. Rev. C **91**, 034301 (2015)
18. D.R. Chakrabarty, V.M. Datar, Suresh Kumar, G. Mishra, E.T. Mirgule, A. Mitra, P.C. Rout, V. Nanal, Deepak Pandit, S. Mukhopadhyay, Srijit Bhattacharya, Phys. Rev. C **85**, 044619 (2012)
19. A.K. Rhine Kumar, P. Arumugam, N. Dinh Dang, I. Mazumdar, Phys. Rev. C **96**, 024322 (2017)
20. G. Bellia, R. Alba, R. Coniglione, A. Del Zoppo, P. Finocchiaro, C. Maiolino, E. Migneco, P. Piattelli, P. Sapienza, N. Frascaria, I. Lhenry, J.C. Roynette, T. Suomijärvi, N. Alamanos, F. Auger, A. Gillibert, D. Pierroutsakou, J.L. Sida, P.R. Silveira Gomes, Nucl. Instrum. Methods Phys. Res. A **329**, 173 (1993)
21. Srijit Bhattacharya, S. Mukhopadhyay, Deepak Pandit, Surajit Pal, A. De, S. Bhattacharya, C. Bhattacharya, K. Banerjee, S. Kundu, T.K. Rana, A. Dey, G. Mukherjee, T. Ghosh, D. Gupta, S.R. Banerjee, Phys. Rev. C **77**, 024318 (2008)
22. T. Suomijärvi, Y. Blumenfeld, P. Piattelli, J.H. Le Faou, C. Agodi, N. Alamanos, R. Alba, F. Auger, G. Bellia, Ph Chomaz, R. Coniglione, A. Del Zoppo, P. Finocchiaro, N. Frascaria, J.J. Gaardhøje, J.P. Garron, A. Gillibert, M. Lamehi-Racti, R. Liguori-Neto, C. Maiolino, E. Migneco, G. Russo, J.C. Roynette, D. Santonocito, P. Sapienza, J.A. Scarpaci, A. Smerzi, Phys. Rev. C **53**, 2258 (1996)
23. H. Nifenecker, J. Blachot, J. Crançon, A. Gizon, A. Lleres, Nucl. Phys. A **447**, 533c (1985)
24. R. Wada, D. Fabris, K. Hagel, G. Nebbia, Y. Lou, M. Gonin, J.B. Natowitz, R. Billerey, B. Cheynis, A. Demeyer, D. Drain, D. Guinet, C. Pastor, L. Vagneron, K. Zaid, J. Alarja, A. Giorni, D. Heuer, C. Morand, J.B. Viano, C. Mazur, C. Ngo, S. Leray, R. Lucas, M. Ribrag, E. Tomasi, Phys. Rev. C **39**, 497 (1989)
25. A. Chbihi, L.G. Sobotka, Z. Majka, D.G. Sarantites, D.W. Stracener, V. Abenante, T.M. Semkow, N.G. Nicolis, D.C. Hensley, J.R. Beene, M.L. Halbert, Phys. Rev. C **43**, 652 (1991)
26. D. Santonocito, P. Piattelli, Y. Blumenfeld, T. Suomijärvi, C. Agodi, N. Alamanos, R. Alba, F. Auger, G. Bellia, Ph Chomaz, M. Colonna, R. Coniglione, A. Del Zoppo, P. Finocchiaro, N. Frascaria, A. Gillibert, J.H. Le Faou, K. Loukachine, C. Maiolino, E. Migneco, J.C. Roynette, P. Sapienza, J.A. Scarpaci, Phys. Rev. C **66**, 044619 (2002)
27. E. Migneco, C. Agodi, R. Alba, G. Bellia, R. Coniglione, A. Del Zoppo, P. Finocchiaro, C. Maiolino, P. Piattelli, G. Raia, P. Sapienza, Nucl. Instr. Methods Phys. Res. A **314**, 31 (1992)
28. D. Santonocito, Y. Blumenfeld, C. Agodi, R. Alba, G. Bellia, R. Coniglione, F. Delaunay, A. Del Zoppo, P. Finocchiaro, F. Hongmei, V. Lima, C. Maiolino, E. Migneco, P. Piattelli, P. Sapienza, J.A. Scarpaci, O. Wieland, Phys. Rev. C **90**, 054603 (2014)
29. D. Santonocito, Y. Blumenfeld, C. Maiolino, C. Agodi, R. Alba, G. Bellia, R. Coniglione, A. Del Zoppo, F. Hongmei, E. Migneco, P. Piattelli, P. Sapienza, L. Auditore, G. Cardella, E. De Filippo, E. La Guidara, C. Monrozeau, M. Papa, S. Pirrone, F. Rizzo, A. Trifiró, M. Trimarchi, H.X. Huang, O. Wieland, Phys. Lett. B **782**, 427 (2018)
30. E. Ramakrishnan, T. Baumann, A. Azhari, R.A. Kryger, R. Pfaff, M. Thoennessen, S. Yokoyama, J.R. Beene, M.L. Halbert, P.E. Mueller, D.W. Stracener, R.L. Varner, R.J. Charity, J.F. Dempsey, D.G. Sarantites, L.G. Sobotka, Phys. Rev. Lett. **76**, 2025 (1996)
31. P. Heckman, D. Bazin, J.R. Beene, Y. Blumenfeld, M.J. Chromik, M.L. Halbert, J.F. Liang, E. Mohrmann, T. Nakamura, A. Navin, B.M. Sherrill, K.A. Snover, M. Thoennessen, E. Tryggestad, R.L. Varner, Phys. Lett. B **555**, 43 (2003)
32. W. Cassing, V. Metag, U. Mosel, K. Niita, Phys. Rep. **188**, 363 (1990)
33. Y.Schutz, G.Martinez, F. M. Marqués, A. Marín, T- Matulewicz, R. W. Ostendorf, P. Bozek, H. Delagrange, J. Díaz, M. Franke, K. K. Gudima, H. Slaváč, R. Holtzmann, P. Latridou, F. Lefévre, H. Löhner, W. Mittig, M. Ploszajczak, J. H. G. van Pol, J. Québert, P. Roussel-Chomaz, A. Schubert, R. H. Siemssen, R. S. Simon, Z. Sujkowski, V. D. Toneev, V. Wagner, H. W. Wilschut, Gy. Wolf, Nucl. Phys. A **622**, 404 (1997)
34. H. Nifenecker, J.A. Pinston, Ann. Rev. Nucl. Part. Sci. **40**, 113 (1990)
35. M. Mattiuzzi, A. Bracco, F. Camera, W.E. Ormand, J.J. Gaardhøje, A. Maj, B. Million, M. Pignanelli, T. Tveter, Nucl. Phys. **A612**, 262 (1997)
36. S.K. Rathi, D.R. Chakrabarty, V.M. Datar, Suresh Kumar, E .T. Mirgule, A. Mitra, V. Nanal, H .H. Oza, Phys. Rev **C67**, 024603–1 (2003)
37. M. Thoennessen, E. Ramakrishnan, J.R. Beene, F.E. Bertrand, M.L. Halbert, D.J. Horen, P.E. Mueller, R.L. Varner, Phys. Rev. **C51**, 3148 (1995)
38. F. Pühlhofer, Nucl. Phys. **A280**, 267 (1977)
39. J.B. Natowitz, R. Wada, K. Hagel, T. Keutgen, M. Murray, A. Makeev, L. Qin, P. Smith, C. Hamilton, Phys. Rev. **C65**, 034618-1 (2002). and references therein
40. I. Diosegi, Phys. Rev. **C64**, 019801 (2001). and references therein
41. W. Dilg, W. Schantl, H. Vonach, M. Uhl, Nucl. Phys. **A217**, 269 (1973)
42. A.V. Ignatyuk, G.N. Smirenin, A.S. Tishin, Sov. J. Nucl. Phys. **21**, 255 (1975)
43. W. Reisdorf, Z. Phys. **A300**, 227 (1981)
44. R.J. Charity, Phys. Rev. **C82**, 014610 (2010)
45. M. Ciemala, M. Kmiecik, M. Krzysiek, A. Maj, K. Mazurek, R. Charity, D. Mancusi, Acta Phys. Pol. **B44**, 611 (2013)
46. M. Ciemala, M. Kmiecik, A. Maj, K. Mazurek, A. Bracco, V.L. Kravchuk, G. Casini, S. Barlini, G. Baiocco, L. Bardelli, P. Bednarczyk, G. Benzoni, M. Bini, N. Blasi, S. Brambilla, M. Bruno, F. Camera, S. Carboni, M. Cinausero, A. Chbihi, M. Chiari, A. Corsi, F.C.L. Crespi, M. D'Agostino, M. Degerlier, B. Fornal, A. Giaz, F. Gramegna, M. Krzysiek, S. Leoni, T. Marchi, M. Matejska-Minda, I. Mazumdar, W. Meczynski, B. Million, D. Montanari, L. Morelli, S. Myalski, A. Nannini, R. Nicolini, G. Pasquali, S. Piantelli, G. Prete, O.J. Roberts, Ch. Schmitt, J. Styczen, B. Szpak,

S. Valdre, B. Wasilewska, O. Wieland, J.P. Wieleczko, M. Zieblinski, J. Dudek, N. Dinh Dang, Phys. Rev. **C91**, 054313 (2015)
47. D.R. Chakrabarty, S. Sen, M. Thoennessen, N. Alamanos, P. Paul, R. Schicker, J. Stachel, J.J. Gaardhøje, Phys. Rev. **C36**, 1886 (1987)
48. P. Heckman, B.B. Back, T. Baumann, M.P. Carpenter, I. Diószegi, D.J. Hofman, T.L. Khoo, S. Mitsuoka, V. Nanal, T. Pennington, J.P. Seitz, M. Thoennessen, E. Tryggestad, R.L. Varner, Nucl. Phys. **A750**, 175 (2005)
49. A. Bracco, F. Camera, Nucl. Phys. **A788**, 205c (2007)
50. O. Wieland, A. Bracco, F. Camera, G. Benzoni, N. Blasi, S. Brambilla, F. Crespi, A. Giussani, S. Leoni, P. Mason, B. Million, A. Moroni, S. Barlini, V.L. Kravchuk, F. Gramegna, A. Lanchais, P. Mastinu, A. Maj, M. Brekiesz, M. Kmiecik, M. Bruno, E. Geraci, G. Vannini, G. Casini, M. Chiari, A. Nannini, A. Ordine, E. Ormand, Phys. Rev. Lett. **97**, 012501 (2006)
51. A. Bracco, F. Camera, O. Wieland, W.E. Ormand, Mod. Phys. Lett. **A22**, 2479 (2007)
52. M.P. Kelly, K.A. Snover, J.P.S. van Schagen, M. Kicińska-Habior, Z. Trznadel, Phys. Rev. Lett. **82**, 3404 (1999)
53. T. Baumann, E. Ramakrishnan, A. Azhari, J.R. Beene, R.J. Charity, J.F. Dempsey, M.L. Halbert, P.F. Hua, R.A. Kryger, P.E. Mueller, R. Pfaff, D.G. Sarantites, L.G. Sobotka, D.W. Stracener, M. Thoenessen, G. Van Buren, R.L. Varner, S. Yokoyama, Nucl. Phys. **A635**, 248 (1998)
54. J.O. Newton, B. Herskind, R.M. Diamond, E.L. Dines, J.E. Draper, K.H. Lindenberger, C. Schück, S. Shih, F.S. Stephens, Phys. Rev. Lett. **46**, 1383 (1981)
55. J.J. Gaardhøje, C. Ellegaard, B. Herskind, S.G. Steadman, Phys. Rev. Lett. **53**, 148 (1984)
56. J.J. Gaardhøje, C. Ellegaard, B. Herskind, R.M. Diamond, M.A. Delaplanque, G. Dines, A.O. Macchiavelli, F.S. Stephens, Phys. Rev. Lett. **56**, 1783 (1986)
57. A. Bracco, F. Camera, M. Mattiuzzi, B. Million, M. Pignanelli, J.J. Gaardhøje, A. Maj, T. Ramsøy, T. Tveter, Z. Zelazny, Phys. Rev. Lett. **74**, 3748 (1995)
58. A. Maj, J.J. Gaardhøje, A. Atac, S. Mitarai, J. Nyberg, A. Virtanen, A. Bracco, F. Camera, B. Million, M. Pignanelli, Nucl. Phys. **A571**, 185 (1994)
59. Y. Alhassid, B. Bush, S. Levit, Phys. Rev. Lett. **71**, 1926 (1988)
60. W.E. Ormand, P.F. Bortignon, R.A. Broglia, A. Bracco, Nucl. Phys. **A614**, 217 (1997)
61. D. Kusnezov, Y. Alhassid, K. A. Snover, Phys. Rev. Lett. **81**, 542 (1998) (and references therein)
62. M. Kmiecik, A. Maj, A. Bracco, F. Camera, M. Casanova, S. Leoni, B. Million, B. Herskind, R.A. Bark, W.E. Ormand, Nucl. Phys. **A674**, 29 (2000)
63. M. Mattiuzzi, A. Bracco, F. Camera, B. Million, M. Pignanelli, J.J. Gaardhøje, A. Maj, T. Ramsøy, T. Tveter, Z. Źelazny, Phys. Lett. **B364**, 13 (1995)
64. F. Camera, A. Bracco, S. Leoni, B. Million, M. Mattiuzzi, M. Pignanelli, A. Maj, M. Kmiecik, R. Bark, J. Bearden, J.J. Gaardhøje, W.E. Ormand, T. Lonnroth, R. Osterbacka, Phys. Rev. **C60**, 014306 (1999)
65. D.R. Chakrabarty, V.M. Datar, Suresh Kumar, E.T. Mirgule, A. Mitra, V. Nanal, R.G. Pillay, P.C. Rout, J. Phys. G: Nucl. Part. Phys **37**, 055105 (2010)
66. V. Baran, A. Bonasera, M. Colonna, M. Di Toro, A. Guarnera, Prog. Part. Nucl. Phys. **38**, 263 (1997)
67. W.E. Ormand, P.F. Bortignon, R.A. Broglia, Nucl. Phys. **A599**, 57c (1996)
68. W.E. Ormand, Nucl. Phys. **A649**, 145c (1999)
69. P. Chomaz, Phys. Lett. **B347**, 1 (1995)
70. F. Camera, A. Bracco, V. Nanal, M.P. Carpenter, F. Della Vedova, S. Leoni, B. Million, S. Mantovani, M. Pignanelli, O. Wieland, B.B. Back, A.M. Heinz, R.V.F. Janssens, D. Jenkins, T.L. Khoo, F.G. Kondev, T. Lauritsen, C.J. Lister, B. McClintock, S. Mitsuoka, E.F. Moore, D. Seweryniak, R.H. Siemssen, R.J. Van Swol, D. Hofmann, M. Thoennessen, K. Eisenman, P. Heckman, J. Seitz, R. Varner, M. Halbert, I. Dioszegi, A. Lopez-Martenz, Phys. Lett. **B560**, 155 (2003)
71. S. Mukhopadhayay, Deepak Pandit, Surajit Pal, Srijit Bhattacharya, A. Dec, S. Bhattacharya, C. Bhattacharya, K. Banerjee, S. Kundu, T.K. Rana, G. Mukherjee, R. Pandey, M. Gohil, H. Pai, J.K. Meena, S.R. Banerjee, Phys. Lett **B709**, 9 (2012)
72. Deepak Pandit, S. Mukhopadhyaya, Surajit Pal, A. Deb, S.R. Banerjee, Phys. Lett **B713**, 434 (2012)
73. M. Kicinska-Habior, K.A. Snover, C.A. Gossett, J.A. Behr, G. Feldman, H.K. Glatzel, J.H. Gundlach, E.F. Garman, Phys. Rev. **C36**, 612 (1987)
74. S. Ceruti, F. Camera, A. Bracco, A. Mentana, R. Avigo, G. Benzoni, N. Blasi, G. Bocchi, S. Bottoni, S. Brambilla, F.C.L. Crespi, A. Giaz, S. Leoni, B. Million, A.I. Morales, R. Nicolini, L. Pellegri, S. Riboldi, O. Wieland, D. Bazzacco, M. Ciemala, E. Farnea, A. Gottardo, M. Kmiecik, A. Maj, D. Mengoni, C. Michelagnoli, V. Modamio, D. Montanari, D. Napoli, F. Recchia, E. Sahin, C. Ur, J.J. Valiente-Dobon, B. Wasilewska, M. Zieblinski, Phys. Rev. **C95**, 014312 (2017)
75. A.K. Rhine Kumar, P. Arumugam, N. Dinh Dang, Phys. Rev. **C90**, 044308 (2014)
76. A.K. Rhine Kumar, P. Arumugam, N. Dinh Dang, Phys. Rev. **C91**, 044305 (2015)
77. A. Bracco, J.J. Gaardhøje, A.M. Bruce, J.D. Garrett, B. Herskind, M. Pignanelli, D. Barnéoud, H. Nifenecker, J.A. Pinston, C. Ristori, F. Schussler, J. Bacelar, H. Hofmann, Phys. Rev. Lett. **62**, 2080 (1989)
78. G. Enders, F.D. Berg, K. Hagel, W. Kühn, V. Metag, R. Novotny, M. Pfeiffer, O. Schwalb, R.J. Charity, A. Gobbi, R. Freifelder, W. Henning, K.D. Hildenbrand, R. Holzmann, R.S. Mayer, R.S. Simon, J.P. Wessels, G. Casini, A. Olmi, A.A. Stefanini, Phys. Rev. Lett. **69**, 249 (1992)
79. J.B. Natowitz, S. Leray, R. Lucas, C. Ngô, E. Tomasi, C. Volant, Z. Phys. **A325**, 467 (1986)
80. H.J. Hofmann, J.C. Bacelar, M.N. Harakeh, T.D. Poelhekken, A. van der Woude, Nucl. Phys. **A571**, 301 (1994)
81. M.P. Kelly, J.F. Liang, A.A. Sonzogni, K.A. Snover, J.P.S. van Schagen, J.P. Lestone, Phys. Rev. **C56**, 3201 (1997)
82. K.A. Snover, Nucl. Phys. **A687**, 337c (2001)
83. K. A. Snover, in Future Directions in Nuclear Physics with $4\pi$ Gamma Detection Systems of the New Generation, edited by J. Dudek and B. Haas, AIP Conf. Proc. No. 259, p. 299 (AIP, New York, 1992)
84. R.J. Vojtech, R. Butsch, V.M. Datar, M.G. Herman, R.L. McGrath, P. Paul, M. Thoennessen, Phys. Rev. **C40**, R2441 (1989)
85. E.F. Garman, K.A. Snover, S.H. Chew, S.K.B. Hesmondhalgh, W.N. Catford, P.M. Walker, Phys. Rev. **C28**, 2554 (1983)
86. M. Kicinska-Habior, K.A. Snover, J.A. Behr, C.A. Gossett, J.H. Gundlach, G. Feldman, Phys. Rev. **C45**, 569 (1992)
87. J.H. Gundlach, K.A. Snover, J.A. Behr, C.A. Gossett, M. Kicinska-Habior, K.T. Lesko, Phys. Rev. Lett. **65**, 2523 (1990)
88. J.J. Gaardhøje, A.M. Bruce, J.D. Garrett, B. Herskind, D. Barnéoud, M. Maurel, H. Nifenecker, J.A. Pinston, P. Perrin, C. Ristori, F. Schussler, A. Bracco, M. Pignanelli, Phys. Rev. Lett. **59**, 1409 (1987)
89. K. Yoshida, J. Kasagi, H. Hama, M. Sakurai, M. Kodama, K. Furutaka, K. Ieki, W. Galster, T. Kubo, M. Ishihara, Phys. Lett. **B245**, 7 (1990)
90. K. Yoshida, J. Kasagi, H. Hama, M. Sakurai, M. Kodama, K. Furutaka, K. Ieki, W. Galster, T. Kubo, M. Ishihara, A. Galonsky, Phys. Rev. **C46**, 961 (1992)
91. J. Kasagi, K. Yoshida, Nucl. Phys. **A557**, 221c (1993)
92. A. Smerzi, A. Bonasera, M. Di Toro, Phys. Rev. **C44**, 1713 (1991)

93. A. Smerzi, M. Di Toro, D.M. Brink, Phys. Lett. **B320**, 216 (1994)
94. A. Bonasera, M. Di Toro, A. Smerzi, D.M. Brink, Nucl. Phys. **A569**, 215c (1994)
95. D.M. Brink, Nucl. Phys. **A519**, 3c (1990)
96. P.F. Bortignon, A. Bracco, D. Brink, R.A. Broglia, Phys. Rev. Lett. **67**, 3360 (1991)
97. J. Kasagi, K. Yoshida, Nucl. Phys. **A569**, 195c (1994)
98. J.H. Le Faou, T. Suomijärvi, Y. Blumenfeld, P. Piattelli, C. Agodi, N. Alamanos, R. Alba, F. Auger, G. Bellia, Ph Chomaz, R. Coniglione, A. Del Zoppo, P. Finocchiaro, N. Frascaria, J.J. Gaardhøje, J.P. Garron, A. Gillibert, M. Lamehi-Racti, R. Liguori-Neto, C. Maiolino, E. Migneco, G. Russo, J.C. Roynette, D. Santonocito, P. Sapienza, J.A. Scarpaci, A. Smerzi, Phys. Rev. Lett. **72**, 3321 (1994)
99. W.E. Ormand, P.F. Bortignon, A. Bracco, R.A. Broglia, Phys. Rev. **C40**, 1510 (1989)
100. P. Piattelli, Y. Blumenfeld, J .H. Le Faou, T. Suomijärvi, C. Agodi, N. Alamanos, R. Alba, F. Auger, G. Bellia, Ph Chomaz, R. Coniglione, A. Del Zoppo, P. Finocchiaro, N. Frascaria, J.J. Gaardhøje, J .P. GArron, A. Gillibert, M. Lamehi-Racti, R. Liguori-Neto, K. Loukachine, C. Maiolino, E. Migneco, J .C. Roynette, D. Santonocito, P. Sapienza, J .A. Scarpaci, Nucl. Phys **A599**, 63c (1996)
101. G. Bellia, P. Finocchiaro, K. Loukachine, C. Agodi, R. Alba, L. Calabretta, R. Coniglione, A. Del Zoppo, C. Maiolino, E. Migneco, P. Piattelli, G. Raciti, D. Rifuggiato, D. Santonocito, P. Sapienza, IEEE Trans. Nucl. Sci. **43**, 1737 (1996)
102. D. Santonocito, Y. Blumenfeld, C. Maiolino, R. Alba, G. Bellia, R. Coniglione, A. Del Zoppo, E. Migneco, P. Piattelli, P. Sapienza, L. Auditore, G. Cardella, E. De Filippo, E. La Guidara, C. Monrozeau, M. Papa, S. Pirrone, F. Rizzo, A. Trifiró, M. Trimarchi, H.X. Huang, O. Wieland, Acta Phys. Pol. **B50**, 451 (2019)
103. A. Musumarra, G. Cardella, A. Di Pietro, S.L. Li, M. Papa, G. Pappalardo, F. Rizzo, S. Tudisco, J.P.S. van Schagen, Nucl. Instr. Methods **A370**, 558 (1996)
104. S. Tudisco, G. Cardella, F. Amorini, A. Anzalone, A. Di Pietro, P. Figuera, F. Giustolisi, G. Lanzalone, Lu Jun, A. Musumarra, M. Papa, S. Pirrone, F. Rizzo, Europhys. Lett. **58**, 811 (2002)
105. F. Amorini, G. Cardella, A. Di Pietro, P. Figuera, G. Lanzalone, Lu Jun, A. Musumarra, M. Papa, S. Pirrone, F. Rizzo, W. Tian, S. Tudisco, Phys. Rev. **C69**, 014608–1 (2004)
106. P. Chomaz, M. Di Toro, A. Smerzi, Nucl. Phys. **A563**, 509 (1993)
107. A. Bonasera, M. Bruno, C.A. Dorso, P.F. Mastinu, Riv. N. Cimento **23** (2000)


**D. Santonocito** is a INFN researcher at the Laboratori Nazionali del Sud (Catania). He got the PhD at the University of Catania and, as post-doc, a Marie Curie fellowship from European Community at the IPN Orsay where he worked with the group of Y. Blumenfeld. His research activities were focused on the study of the Giant Dipole Resonances and the reaction dynamics at intermediate energies. From 2008 to 2014 he has been national responsible of the research group LNS-STREAM at the LNS. He has been collaborating with Yorick Blumenfeld since the 1990s to study the hot GDR with the MEDEA detector.

**Y. Blumenfeld** is a CNRS research director at IJCLab (formerly IPN Orsay). He was a visiting scientist at LBL Berkeley and NSCL MSU and acted as group leader and spokesperson for the ISOLDE facility at CERN from 2008 to 2012. His expertise lies in the experimental study of nuclear reactions and his focus has been on Giant Resonance excitation and decay and on direct reactions induced by radioactive beams. He has been collaborating with Domenico Santonocito since the 1990s to study the hot GDR with the MEDEA detector, at first at GANIL and subsequently at LNS Catania.